NUMERICAL SOLUTIONS OF OPTIMAL FIXED-THRUST

PLANETOCENTRIC SPIRAL TRAJECTORIES (LOW-THRUST)

Submitted by: Garwood W. Bacon
Garwood W. Bacon

Approved by: M Handelsman

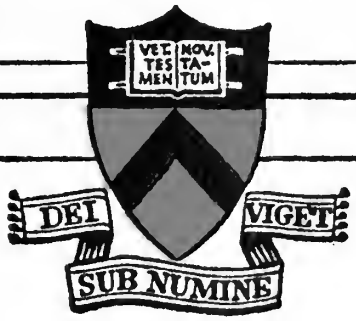


PRINCETON UNIVERSITY

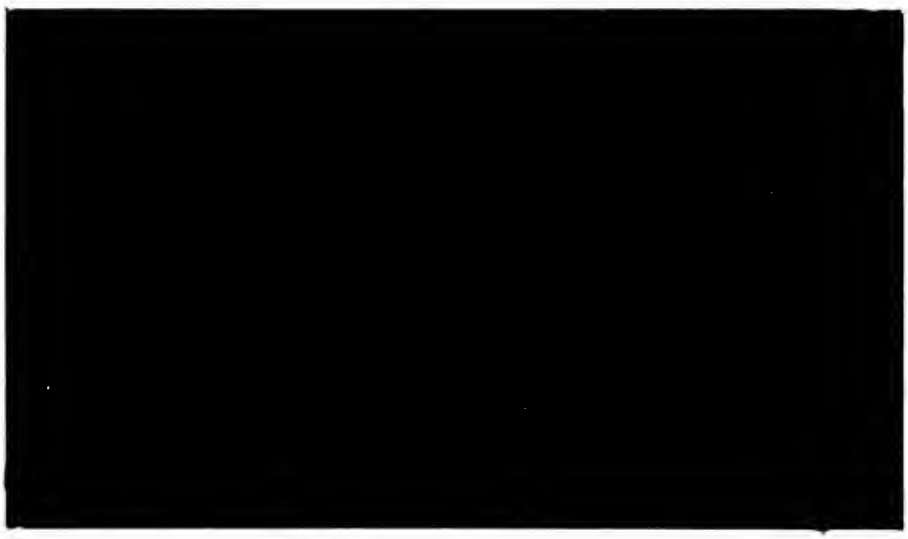

# NUMERICAL SOLUTIONS OF OPTIMAL FIXED-THRUST PLANETOCENTRIC SPIRAL TRAJECTORIES (LOW-THRUST)

March 1970

A thesis submitted to the Department of Aerospace and Mechanical Sciences of Princeton University in partial fulfillment of the requirement for the degree of Master of Science in Engineering.

PRINCETON UNIVERSITY
Princeton, New Jersey

## SUMMARY

The methods of Hamilton and Lagrange in the calculus of variations are employed to optimize planetocentric orbital transfers using fixed-thrust engines, where the thrust acceleration $<<$ local gravitational acceleration. The equations were derived for minimum time transfers. However, since fixed-thrust engines are used, the minimum fuel problem is solved simultaneously. Numerical solutions are obtained by integrating the optimized differential equations of motion for the problem, the actual integrations being performed by an IBM 360/30 computer. The numerical integrations result in optimal spiral trajectories representing orbital transfers between specified coplanar, co-axial ellipses, with the optimal thrust angle being calculated at all points along the trajectories. For an orbital transfer at the planet Mars, the low fixed-thrust system yields a significant increase in the amount of payload that can be delivered into the desired final orbit compared with a transfer accomplished by an impulsive (high thrust) chemical rocket propulsion system. However, the time required to achieve the transfer is necessarily longer in the low-thrust case. It is then necessary to examine the trade-off between the increase in payload and the extra transfer time to determine whether or not the fixed-thrust system is desirable.

ACKNOWLEDGMENTS

The author wishes to express his gratitude for the continued support and encouragement from The Aerospace Systems Laboratory of the Department of Aerospace and Mechanical Sciences, Princeton University.

Special thanks are extended to Dr. Morris Handelsman whose original work formed the basis for this thesis. His guidance and assistance were invaluable to its successful completion.

Special thanks are also extended to Mr. J. P. Layton whose constant encouragement and helpful criticism are greatly appreciated. He contributed many constructive ideas while reviewing the text.

Many other members of The Aerospace Systems Laboratory contributed their time and efforts. Mr. John H. Campbell aided in programming the solutions and Mrs. Alexandra B. Shulzycki programmed the flow charts. Miss Frances Allison provided secretarial assistance and Miss Linda Levitcher typed the manuscript. Dr. P. M. Lion and Mr. J. F. Swale gave their very helpful ideas through several group discussions on the thesis topic.

The author takes this opportunity to thank them all.

This thesis carries T-901 in the records of the Department of Aerospace and Mechanical Sciences.

CONTENTS

CONTENTS (continued)

LIST OF TABLES

LIST OF FIGURES

LIST OF FIGURES (continued)

# TABLE OF SYMBOLS

$a$ = semi-major axis of ellipse

$e$ = eccentricity

$E$ = eccentric anomaly

$t$ = time elapsed

$\alpha$ = thrust (steering) angle, measured with reference to local horizontal

$A$ = thrust acceleration

$k$ = central body gravitational constant = GM

$f_1, f_2$ = defined by equations (30) and (31), respectively

$f_o, \beta$ = defined by equation (27)

$X_1, X_2$ = state variables a, e , respectively

$\lambda_i$ = adjoint variables

$G$ = function to be optimized

$H$ = Hamiltonian function

$\xi$ = defined by equation (40)

$X, Y, Z$
$W, N, D$ = defined by equations (44) through (49)

$v_j$ = rocket exhaust velocity

$r_{ep}$ = radius of ellipse at periapse

$v_{p_i}$ = initial incoming parabolic velocity at periapse

$v_{ep}$ = elliptical orbit velocity at periapse

$m_{c1}$ = mass into final circular orbit using chemical retro propulsion

$m_{c2}$ = mass into final circular orbit by solar electric spiral process

$v_c$ = circular orbital velocity

$\Delta v_c$ = defined by equation (88)

TABLE OF SYMBOLS (continued)

$\Delta m_{cl}$ = fuel mass required for chemical retro directly into final circular orbit

$m_{ell}$ = initial mass in ellipse

$F$ = thrust magnitude

$I_{sp}$ = specific impulse

$g$ = local gravitational acceleration

$|\dot{m}|$ = fuel mass flow rate

$\Delta m_s$ = fuel expended while spiraling

Subscripts

o = initial

f = final

ell = ellipse

# I. INTRODUCTION

As we explore the space around us, we look for ways of doing things more efficiently, ways to save money, and ways to put heavier payloads into orbit at the same or less cost than is presently possible. One feasible way of accomplishing this is through the use of solar-electro-static or nuclear-electro-static propulsion systems. They require much less fuel (weight-wise) than chemical rocket engines, have much higher specific impulses, and can result in considerable increases in final payload delivered. They do, however, require more time to achieve the same orbital maneuvers because of the much lower thrust inherent in these type of systems.

Considerable research on optimal low thrust maneuvers has been done in recent years. A large part of this work has been done by T. N. Edelbaum. He has published papers which contain solutions for optimum power-limited transfer and rendezvous between arbitrary coplanar and coaxial elliptic and circular orbits. The assumptions involved in the development are 1) the thrust acceleration is much smaller than the local gravitational acceleration. 2) the propulsion system is power-limited, i.e., it operates at constant exhaust power with a variable thrust magnitude inversely proportional to the exhaust velocity. 3) the direction and magnitude of the thrust, both of which are assumed to be completely variable, is to be determined as a function of time so as to minimize the fuel consumption for a fixed total transfer time. Edelbaum has also developed an analytic solution for fixed thrust systems, but this is only applicable to transfers between almost circular orbits, for small

changes in $a$ and $e$, and for large changes in $a$ and $i$ (orbital plane inclination)(Reference 1, 2, 3).

This thesis addresses the problem of optimizing fixed, low-thrust orbital transfers with large changes in $a$ and $e$. Based upon a Lagrange-Hamilton formulation developed by Dr. M. Handelsman (Reference 4) the numerical solution of optimized transfer trajectories is performed by computer. The solutions involve the optimization of planetocentric transfers between coplanar, coaxial ellipses or circles of specified characteristics, with no time constraint. Because of the relatively small fuel expenditure in these transfers, it is possible to replace "fixed thrust" with "fixed thrust acceleration" throughout the entire transfer with little error. Solar electric engines lose a certain amount of thrust as their distance from the sun increases; this could hardly be considered constant thrust in heliocentric space. But, since the problem has been limited to a planetocentric study, the thrust of the solar electric engine can be assumed to be constant within the planetocentric space.

By fixed thrust, it is meant that the thrust magnitude is constant and that the engine remains turned on at all times during the transfer. The problem then remains, where to point the thrust at all times. Now, there are many factors which could be optimized in an orbital transfer of this type. In this thesis two separate phenomena were optimized. First, orbital transfers were optimized for minimum time using fixed thrust engines. Since the thrust is fixed, and, therefore, continuous, then a minimum time transfer would also be a minimum fuel transfer, the amount of fuel expended being directly proportional to the length of time the engine is turned on. Secondly,

orbital transfers were optimized for minimum E (eccentric anomaly); in other words, transfers were achieved to the desired orbit in the least amount of revolutions. The significance of this type of transfer trajectory is that it lends considerable insight into the minimum time, minimum fuel problem.

The problem formulation involves deriving the perturbation equations of motion for fixed thrust engines of low, constant magnitude, and then optimizing them for minimum time and minimum E using Hamilton , Lagrange, and Mayer techniques in the calculus of variations. (Reference 4). After being optimized for minimum time and minimum E respectively, the differential equations are set up to solve for the optimum thrust angle necessary at all times to achieve the optimized transfers. These sets of equations are then solved by numerical integration,in this case on an IBM 360-30 computer system. An analytic solution is not available at present because of the inability to solve for Langrangian multipliers. This is the reason for the numerical approach.

The basic assumptions follows:

1) The thrust acceleration is much less than the local gravitational acceleration. ($A \ll g$).

2) Continuous, fixed-magnitude thrust.

3) Relatively small total fuel consumption; therefore, for the sake of simplicity, the thrust acceleration is assumed to be essentially constant over the transfer. That is, constant thrust magnitude is taken as synonymous with constant thrust acceleration. (A program modification to incorporate the changes in thrust acceleration due to fuel depletion is simple to implement).

A description of the problem and its formulation follows.

## II. DESCRIPTION OF PROBLEM

An initial elliptic orbit is assumed about a planet or any other body which has an inverse-square gravitational field. The ellipse has specifications $(a_o, e_o)$, where $a_o$ is the initial semi-major axis and $e_o$ is the initial eccentricity. The problem then is to transfer optimally to a desired final coaxial, coplanar ellipse with specifications $(a_f, e_f)$. See figure 1. This is accomplished by turning on the engine at the initial ellipse periapse and letting the optimally-directed fixed thrust program guide the vehicle along a spiral trajectory until the final ellipse is obtained. The engine is then shut off and the spacecraft is in its new orbit, the transfer having been conducted in minimum time and fuel expenditure or in the least amount of revolutions, depending upon which program is used. The numerical results show that the minimum time transfers always take more revolutions than the minimum E transfers, and the minimum E transfers always take more time than the minimum time transfers. This is as expected and lends considerable support to the calculations.

Each particular transfer is determined by the selection of the initial Lagrangian multiplers. Given an initial ellipse, different sets of inital Lagrangian multipliers will cause the vehicle to transfer to different ellipses. Since we have no analytic way of picking these multipliers at present, many cases are run to cover a wide range of transfers from given initial orbits.

The formulation of both the minimum time and minimum E equations follows as the first phase of the problem solution.

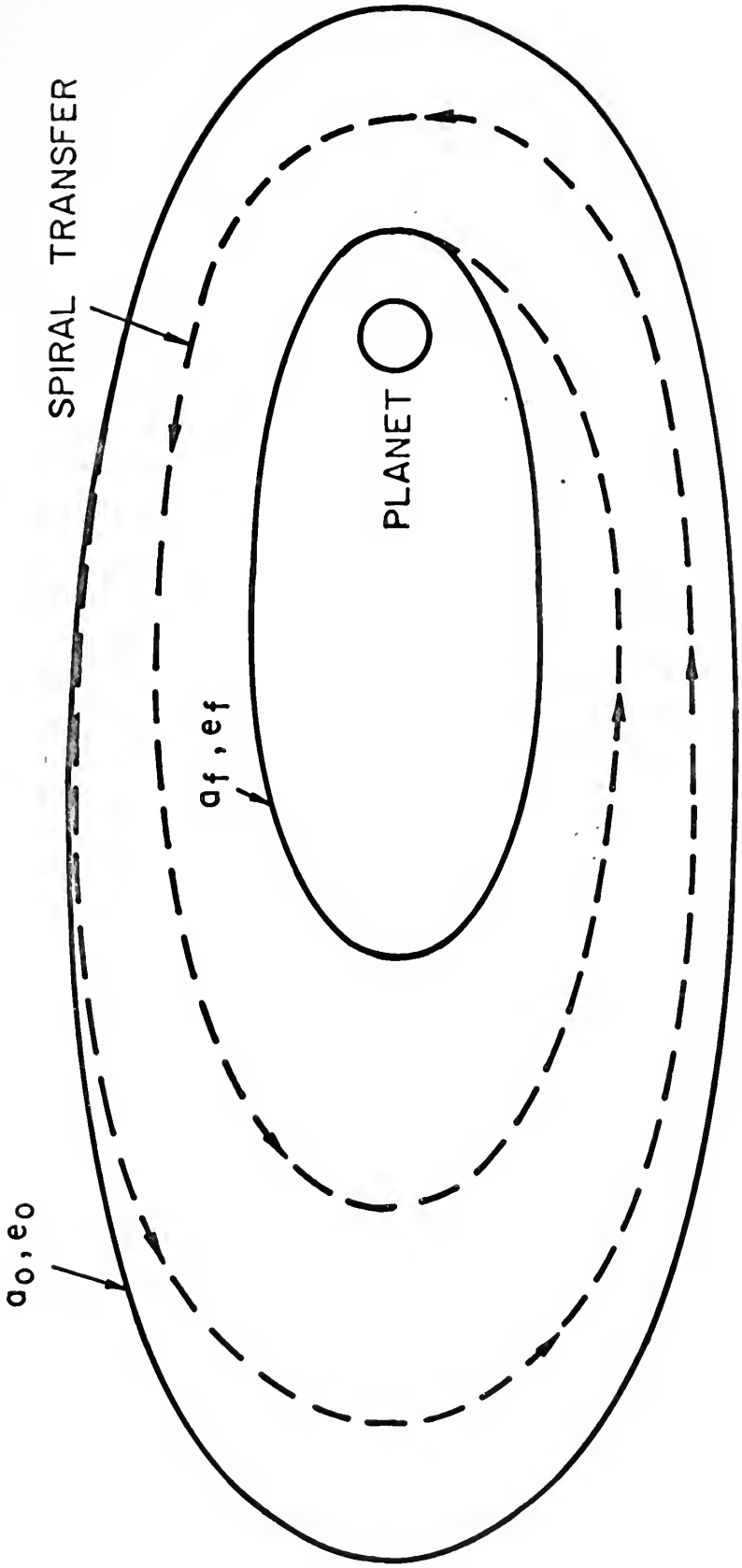


TYPICAL SPIRAL TRANSFER

FIGURE 1

## III. LAGRANGE FORMULATION IN VARIABLE E

### A. Orbital Perturbation Equations

The general orbital perturbation equations in terms of radial tangential thrust forces, S and T respectively, shown in Figure 2, are as follows: (Reference 5)

Some useful relations follow:

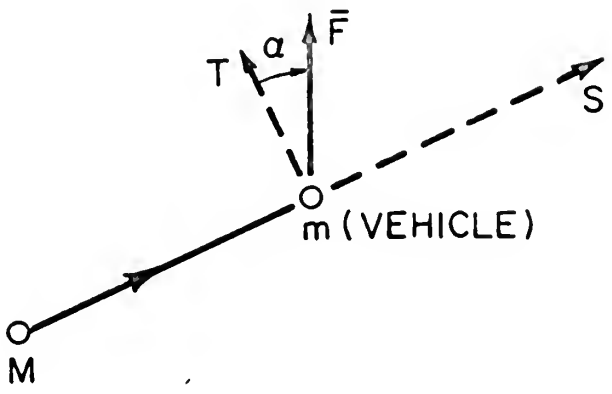


FIGURE 2.
Vehicle Force Vectors

$$\dot{a} = \frac{da}{dt} = \frac{2}{n\sqrt{1-e^2}} \left(S\, e \sin f + T \frac{p}{r}\right) \tag{1}$$

$$\dot{e} = \frac{de}{dt} = \frac{\sqrt{1-e^2}}{n\,a} \left[S \sin f + T(\cos E + \cos f)\right] \tag{2}$$

Using:

$$\cos E + \cos f = \frac{1}{e}\left(\frac{p}{r} - \frac{r}{a}\right)$$

$p = a(1-e^2)$

$f =$ true anomaly $= \theta$

$E =$ eccentric anomaly

Equations (1) and (2) become:

$$\dot{a} = \frac{2e\{\sin f\}S}{n\sqrt{1-e^2}} + \frac{2a\sqrt{1-e^2}}{rn} T \tag{3}$$

$$\dot{e} = \frac{\sqrt{1-e^2}\ \sin f}{na} S + \frac{\sqrt{1-e^2}}{a^2 ner}\left[a^2(1-e^2) - r^2\right] T \tag{4}$$

$$n^2a^3 = \gamma = \mu = ,k = GM \tag{5}$$

$$n = \sqrt{k/a^3} = 2\pi\ /_{(\text{period})} \tag{6}$$

$$S = F_{NORMAL/m} = F \sin\alpha\ /m \tag{7}$$

$$T = F_{TANG./m} = F \cos\alpha\ /m \tag{8}$$

For an ellipse:

$$r = \frac{a\ (1-e^2)}{1+e\ \cos\ f} \tag{9}$$

Through substitution and simplification equation (3) yields:

$$\frac{\dot{a}}{a} = \frac{2}{\sqrt{1-e^2}}\ \frac{F}{m}\ \sqrt{\frac{a}{k}}\left[e \sin\theta + \sin\alpha + (1 + e\cos\theta)\cos\alpha\right] \tag{10}$$

Similarly, equation (4) yields:

$$\dot{e} = \sqrt{1-e^2}\ \frac{F}{m}\sqrt{\frac{a}{k}}\left[\sin\theta\sin\alpha + \frac{2\cos\theta + e(1+\cos^2\theta)\cos\alpha}{1+e\cos\theta}\right] \tag{11}$$

Next, it is desired to write equations (10) and (11) in terms of the eccentric anomaly E. The following relations between E and $\theta$ are used (Reference 6):

$$\sin\theta = \frac{1+e\cos\theta}{\sqrt{1-e^2}}\ \sin E \tag{12}$$

$$1+e\cos\theta = \frac{1-e^2}{1-e\cos E} \tag{13}$$

$$\therefore\ \sin\theta = \frac{\sqrt{1-e^2}\sin E}{1-e\cos E} \tag{14}$$

$$\cos\theta = \frac{\cos E - e}{1-e\cos E} \tag{15}$$

$$r = \frac{P}{1+e\cos\theta} = \frac{a(1-e^2)}{\frac{1-e^2}{1-e\cos E}} = a(1-e\cos E) \tag{16}$$

$$1+e\cos\theta = \frac{1-e^2}{1-e\cos E} \tag{17}$$

$$\sin E = \frac{r}{p}\ \sin\theta \tag{18}$$

$$d\theta = \frac{\sqrt{1-e^2}}{1-e\cos E}\ dE \tag{19}$$

B. Comparison with Edelbaum's Equations

Substituting equations (12-19), equations (10) and (11) can be written in terms of E:

$$\frac{\dot{a}}{a} = \frac{2F}{(1-e\cos E)m}\left[e\sin\alpha\sin E + \cos\alpha\sqrt{1-e^2}\right] \tag{20}$$

$$\dot{e} = \frac{F}{(1-e\cos E)m}\left[(1-e^2)\sin E\sin\alpha + \sqrt{1-e^2}\,(2\cos E - e\cos^2 E - e)\cos\alpha\right] \tag{21}$$

Equations (20) and (21) agree with Edelbaum's equations for low thrust perturbation (Reference 1).

Since

$$dt = dE\sqrt{\frac{a^3}{k}}\,(1-e\cos E) \tag{22}$$

equations (20) and (21) become:

$$\frac{da}{dE} = \frac{2Aa^3}{k}\left[e\sin E\sin\alpha + \sqrt{1-e^2}\cos\alpha\right] \tag{23}$$

$$\frac{de}{dE} = \frac{Aa^2}{k}\left[(1-e^2)\sin E\sin\alpha + \sqrt{1-e^2}\,(2\cos E - e\cos^2 E - e)\cos\alpha\right] \tag{24}$$

Since we are optimizing the thrust angle for minimum flight time the following integral is minimized:

$$t_f = \int_{E_o}^{E_f}\sqrt{a^3/k}\,(1-e\cos E)\,dE \tag{25}$$

This is of the form (Reference 4, 7)

$$t_f = \int_{E_o}^{E_f} f_o\,(X_1, X_2, E)\,dE \tag{26}$$

where:

$$f_o \equiv \beta = \sqrt{a^3/k}\,(1-e\cos E) \tag{27}$$

$$X_1 = a; \quad X_2 = e \tag{28}$$

C. Employing the Hamiltonian

To find the minimum extremal, we write the Hamiltonian for this system of equations,

$$H = -f_o + \sum_{i=1}^{2} \lambda_i\,(E)\,f_i\ , \tag{29}$$

where

$$f_1 = \frac{dX_1}{dE} = \frac{da}{dE} \tag{30}$$

$$f_2 = \frac{dX_2}{dE} = \frac{de}{dE} \tag{31}$$

The independent variable is the eccentric anomaly E. Substituting into H:

$$H = -\sqrt{a^3/k}\,(1-e\cos E) + \lambda_a \frac{da}{dE} + \lambda_e \frac{de}{dE} \tag{32}$$

Substituting for $\frac{da}{dE}$ and $\frac{de}{dE}$ :

$$H = -\sqrt{a^3/k}\ (1-e\cos E) + \lambda_a \frac{2Aa^3}{k}\left[e\sin E\sin\alpha + \sqrt{1-e^2}\cos\alpha\right] + \lambda_e \frac{Aa^2}{k}\left[(1-e^2)\sin E\sin\alpha + \sqrt{1-e^2}\,(2\cos E - e\cos^2 E - e)\cos\alpha\right] \quad (33)$$

D. Euler-Lagrange Equations for Adjoint Variables

The following are the Euler-Lagrange equations for the adjoint variables $\lambda_i$ :

$$\frac{d\lambda_i}{dE} = -\frac{\partial H}{\partial X_i} \quad (i = 1,2) \quad (34)$$

Expanding equation (34):

$$\frac{d\lambda_a}{dE} = -\left(\lambda_a \frac{\partial f_1}{\partial a} + \lambda_e \frac{\partial f_2}{\partial a}\right) + \frac{1}{\beta}\left(\lambda_a f_1 + \lambda_e f_2\right)\frac{\partial \beta}{\partial a} \quad (35)$$

$$\frac{d\lambda_e}{dE} = -\left(\lambda_a \frac{\partial f_1}{\partial e} + \lambda_e \frac{\partial f_2}{\partial e}\right) + \frac{1}{\beta}\left(\lambda_a f_1 + \lambda_e f_2\right)\frac{\partial \beta}{\partial e} \quad (36)$$

E. Transversality Condition

Next, the transversality condition,

$$\left[-H dE + \lambda_i\, dX_i\right]_o^f = 0 \quad (37)$$

which is to be evaluated using the boundary conditions:

$$t = 0: \quad a = a_o, \quad e = e_o, \quad E_o = 0 \tag{38}$$

$$t = t_f: \quad a = a_f, \quad e = e_f, \quad E_f = \text{OPEN} \tag{39}$$

The choice $E_o = 0$ is made for convenience; this is the periapse point, the usual choice for the initial retro-impulse into a bound planetocentric elliptic orbit from an incoming hyperbolic trajectory.

Combining equations (37), (38), and (39),

$$\lambda_a f_1 + \lambda_e f_2 - \beta \equiv \xi = 0 \text{ (at } t=t_f) \tag{40}$$

F. Control Equation for Optimal Thrust Angle

Equation (40) is a necessary condition for a transfer to be optimized for minimum time (and fuel). For the optimal thrust angle $\alpha$ ,

$$\frac{\partial H}{\partial \alpha} = 0 = \lambda_a \frac{\partial f_1}{\partial \alpha} + \lambda_e \frac{\partial f_2}{\partial \alpha} \tag{41}$$

which becomes

$$0 = \frac{\lambda_a 2Aa^3}{k} \left[e \sin E \cos \alpha - \sqrt{1-e^2} \sin \alpha\right] +$$

$$\frac{\lambda_e Aa^2}{k} \left[(1-e^2) \sin E \cos \alpha - \sqrt{1-e^2} (2 \cos E - e \cos^2 E - e) \sin \alpha\right] \tag{42}$$

Divide through by $\cos\alpha$ and solve for $\tan\alpha$ :

$$\tan\alpha = \frac{2a\,\lambda_a\, e \sin E + \lambda_e\,(1-e^2)\sin E}{2a\,\lambda_a\sqrt{1-e^2} + \lambda_e\sqrt{1-e^2}\,(2\cos E - e\cos^2 E - e)} \tag{43}$$

To simplify the equation for computer programming purposes let:

$$X \equiv e \sin E \tag{44}$$

$$Z \equiv (1-e^2)\sin E \tag{45}$$

$$Y \equiv \sqrt{1-e^2} \tag{46}$$

$$W \equiv \sqrt{1-e^2}\,(2\cos E - e\cos^2 E - e) \tag{47}$$

$$N \equiv 2a\,\lambda_a X + \lambda_e Z \tag{48}$$

$$D \equiv 2a\,\lambda_a Y + \lambda_e W \tag{49}$$

Substituting into equation (41):

$$\tan\alpha = \frac{2a\,\lambda_a X + \lambda_e Z}{2a\,\lambda_a Y + \lambda_e W} \equiv \frac{N}{D} \tag{50}$$

This is the control equation for the optimal thrust angle $\alpha$ . The step variable of integration is E. Time of transfer (t) is determined by integration of equation (22) which can be written:

$$\frac{dt}{dE} = \frac{1}{\beta} \tag{51}$$

Thus, we now have sufficient equations for numerical solutions for different transfers, depending on the values assigned to $\lambda_{a_o}$ and $\lambda_{e_o}$. The problem is next solved using the Mayer formulation to develop an alternate but equivalent set of equations.

## IV. MAYER FORMULATION IN VARIABLE t

The Mayer formulation of the problem proceeds as follows:

$$\frac{dX_i}{dt} = f_i(X_i, u_j, t) \tag{52}$$

Where:

$$X_1 = a, X_2 = e, X_3 = E, u_1 = \alpha \tag{53}$$

The independent variable now is t rather than E as in the Lagrange formulation; here we minimize the value of $t_f$, which will be called G. Thus:

$$G = t_f \tag{54}$$

### A. Hamiltonian and Euler-Lagrange Equations

The Hamiltonian is different and does not contain $f_o$:

$$H = \sum_{i=1}^{3} \lambda_i(t) f_i \tag{55}$$

The Euler-Lagrange equations for the adjoint variables $\lambda_i$ are

$$\frac{d\lambda_i}{dt} = -\frac{\partial H}{\partial X_i} \tag{56}$$

Thus:

$$\frac{d\lambda_a}{dt} = -\frac{1}{\beta}\left(\lambda_a \frac{\partial f_1}{\partial a} + \lambda_e \frac{\partial f_2}{\partial a}\right) + \frac{1}{\beta^2}\left(\lambda_a f_1 + \lambda_e f_2 + \lambda_E\right)\frac{\partial \beta}{\partial a} \tag{57}$$

$$\frac{d\lambda_e}{dt} = -\frac{1}{\beta}\left(\lambda_a \frac{\partial f_1}{\partial e} + \lambda_e \frac{\partial f_2}{\partial e}\right) + \frac{1}{\beta^2}\left(\lambda_a f_1 + \lambda_e f_2 + \lambda_E\right)\frac{\partial \beta}{\partial e} \tag{58}$$

$$\frac{d\lambda_E}{dt} = -\frac{1}{\beta}\left(\lambda_a \frac{\partial f_1}{\partial E} + \lambda_e \frac{\partial f_2}{\partial E}\right) + \frac{1}{\beta^2}\left(\lambda_a f_1 + \lambda_e f_2 + \lambda_E\right)\frac{\partial \beta}{\partial E} \tag{59}$$

B. Control Equation for Optimal Thrust Angle

For the optimal thrust angle:

$$\frac{\partial H}{\partial \alpha} = 0 = \lambda_a \frac{\partial f_1}{\partial \alpha} + \lambda_e \frac{\partial f_2}{\partial \alpha} \tag{60}$$

Equations (57), (58), and (60) are identical to equations (35), (36), and (41), using $dE = \frac{1}{\beta}\, dt$. Thus, the equation for $\tan \alpha$ is the same as equation (50):

$$\tan \alpha = \frac{2a\,\lambda_a X + \lambda_e Z}{2a\,\lambda_a Y + \lambda_e W} \equiv \frac{N}{D} \tag{61}$$

Also, since $t$ is not explicit in equation (52), the Hamiltonian is a constant:

$$H = \frac{\lambda_a f_1 + \lambda_e f_2 + \lambda_E}{\beta} = \text{CONSTANT} \tag{62}$$

C. Transversality Condition

The transversality condition is now

$$\left[-H dt + \lambda_i dX_i\right]_o^f + dG = 0 \tag{63a}$$

Therefore

$$\left[-H dt + \lambda_a da + \lambda_e de + \lambda_E dE\right]_o^f + dt_f = 0 \tag{63b}$$

Applying the boundary conditions from equations (38) and (39),

$$dt_o,\ da_o,\ de_o,\ dE_o,\ da_f,\ de_f = 0 \tag{63c}$$

$$-Hdt_f + \lambda_{E_f}\, dE_f + dt_f = 0 \tag{63d}$$

Hence, since $E_f$ is unspecified,

$$\lambda_{E_f} \equiv \lambda_E(t_f) = 0 \tag{64}$$

and since $t_f$ is also unspecified,

$$-Hdt_f + dt_f = 0 \tag{65}$$

which yields

$$H = 1 \tag{66}$$

Combining equations (62), (64) and (66)

$$\frac{\lambda_a f_1 + \lambda_e f_2 + \lambda_E}{\beta} = 1 \qquad \text{(all } t\text{)} \tag{67}$$

and:

$$\xi \equiv \lambda_a f_1 + \lambda_e f_2 - \beta = 0 \quad (t = t_f) \tag{68}$$

Using equations (67) and (68) the Euler-Lagrange system of three equations (57), (58) and (59) can be reduced to the following two equations:

$$\beta \frac{d\lambda_a}{dt} = \frac{\partial \beta}{\partial a} - \left( \lambda_a \frac{\partial f_1}{\partial a} + \lambda_e \frac{\partial f_2}{\partial a} \right) \tag{69}$$

$$\frac{d\lambda_e}{dt} = \frac{\partial \beta}{\partial e} - \left( \lambda_a \frac{\partial f_1}{\partial e} + \lambda_e \frac{\partial f_2}{\partial e} \right) \tag{70}$$

The solution of equations

$$\frac{da}{dt} = \frac{f_1}{\beta} \tag{71}$$

$$\frac{de}{dt} = \frac{f_2}{\beta} \tag{72}$$

$$\frac{dE}{dt} = \frac{1}{\beta} \tag{73}$$

together with equations (68), (69) and (70) is obtained numerically by choosing initial values as follows:

$$t_o = 0,\ a_o,\ e_o,\ E_o = 0,\ \lambda_a(0),\ \lambda_e(0) \tag{74}$$

This requires guessing of values for $\lambda_a(0)$ and $\lambda_e(0)$ since there is at present no analytic way of choosing them. They must be chosen so that the numerical integration yields the required set of final values as follows:

$$a = a_f,\quad e = e_f,\quad \xi_f = 0 \tag{75}$$

## V. THE MINIMUM E PROBLEM

As mentioned earlier, the minimum E problem sheds some light on the minimum t problem. We now will minimize the final E (number of turns going from $a_o$, $e_o$, $E_o = 0$ to $a_f$, $e_f$).

### A. Hamiltonian and Euler-Lagrange Equations

Using equations (30) and (31) minimize $G = E_f$. The Hamiltonian is

$$H = \lambda_a f_1 + \lambda_e f_2 \tag{76}$$

The Euler-Lagrange equations are

$$\frac{d\lambda_a}{dE} = -\frac{\partial H}{\partial a} = -\left(\lambda_a \frac{\partial f_1}{\partial a} + \lambda_e \frac{\partial f_2}{\partial a}\right) \tag{77}$$

$$\frac{d\lambda_e}{dE} = -\frac{\partial H}{\partial e} = -\left(\lambda_a \frac{\partial f_1}{\partial e} + \lambda_e \frac{\partial f_2}{\partial e}\right) \tag{78}$$

These are different from the Euler-Lagrange equations for minimum t optimization.

### B. Control Equation for Optimal Thrust Angle

For the optimum thrust angle:

$$\frac{\partial H}{\partial \alpha} = 0 = \lambda_a \frac{\partial f_1}{\partial \alpha} + \lambda_e \frac{\partial f_2}{\partial \alpha} \tag{79}$$

C. Transversality Condition

Now, writing the transversality equation,

$$\left[-HdE + \lambda_i dX_i\right]_o^f + dG = 0 \tag{80a}$$

where

$$dG = dE_f \tag{80b}$$

and expanding equation (80a)

$$-Hd\overset{o}{\nearrow}{}_o - HdE_f + \lambda_a d\overset{o}{\nearrow}{}_o + \lambda_a d\overset{o}{\nearrow}{}_f + \lambda_e d\overset{o}{\nearrow}{}_o + \lambda_e d\overset{o}{\nearrow}{}_f + dE_f = 0 \tag{80c}$$

Therefore

$$- HdE_f + dE_f = 0 \tag{80d}$$

which yields

$$H_f = 1 = \lambda_a f_1 + \lambda_e f_2 \quad (\text{at } E = E_f) \tag{80e}$$

## VI. TRAJECTORY ANALYSIS

### A. Comparison of Minimum t and Minimum E Trajectories

Equation (80e) is significant; it means that any pair of initial $\lambda$'s ($\lambda_{a_o}$ , $\lambda_{e_o}$) will automatically generate minimum E trajectories terminating at any $a_f$ , $e_f$ , and $E_f$ . This is so because the condition of equation (80e) can always be met simply by scaling the $\lambda$'s . Note that equations (77) and (78) are both linear in the $\lambda$'s and that the optimal thust angle control equation (79) relies only on the ratio of $\lambda_a/\lambda_e$ and not on their separate magnitudes. Automatic satisfaction of equation (80e) makes it easy to calculate minimum E trajectories and to construct a graphical representation of minimum E transfers on an e/a plane.

Consequently, many transfer trajectories are generated which optimize E , and also some which optimize t . These optimal orbital transfers can be seen in Figure 3, which is a graph of e vs $a/a_o$ . It shows both minimum t and minimum E trajectories which are generated from the same initial orbit around Venus. These particular transfers concern a problem incorporating solar-electric orbiters around the planet Venus. (The thrust acceleration used in the calculations is $5\text{x}10^{-3}$ $m/s^2$). The initial gravitational acceleration is about 0.8 $m/s^2$; thus the basic assumption that $A \ll g$ is satisfied.

In an actual case the value of thrust acceleration would be about 1/25 of $5\text{x}10^{-3}$ $m/s^2$. However, the value of $5\text{x}10^{-3}$ is used for numerical calculations in order to speed up the trajectory and computer times, and thus reduce computer costs. Thus all calculated times must be scaled up by a factor of 25 to achieve a more realistic mission time.

Figure 4 shows minimum E trajectories only, with lines of constant t and E superimposed. Examination of the minimum t and minimum E trajectories readily discloses that orbital transfers from one point on the graph to another are accomplished in the least time by following the minimum t path and in the least total revolutions by following the minimum E path. Figure 5 shows the minimum t trajectories superimposed on the constant t and E lines of Figure 4. The minimum E trajectories are omitted for clarity's sake.

The actual calculated orbital elements oscillate over each turn, as illustrated by curve 1A in Figure 5. For simplicity, the remaining curves are constructed by drawing a smooth curve through the values of the orbital elements of each turn at $E = 2n\pi$ ($n = 0, 1, 2, \ldots$). Curve 1A shows the exact path of a minimum t trajectory. It is obviously an oscillatory type motion, which is much more pronounced here than it would normally be due to the increased thrust acceleration (25 times greater than normal). With the actual thrust of about $2 \times 10^{-4}$ $m/s^2$ the oscillations would adhere much more closely to the average path depicted by the heavy dotted lines - (curve 1B) in Figure 5. The minimum t trajectories, which are also minimum fuel trajectories here, are very similar to the minimum fuel trajectories calculated with variable thrust by Edelbaum.*

B. Rotation of Line of Apsides

When considering optimal orbital transfers between coaxial orbits, one wishes to maintain the same line of apsides. Since this program is designed

---

*See Section VIII.

to change only $a$ and $e$, no change in the line of apsides is expected. A close watch is kept of the change in apsidal line angle throughout all orbital transfers and it is verified through calculated results that such changes are small and relatively insignificant. In some instances a change of up to one degree in the line of apsides is detected over a transfer involving up to about 50 revolutions, i.e., one degree change in 18,000 degrees of revolution.

Several points along curves 1B and 2 in Figure 5 indicated along with the flight time and eccentric anomaly elapsed at each position. Discussion of these points follows.

Point J. Following a minimum time trajectory, the vehicle arrives at point J after 3.03 days' time and 37.69 radians of revolution. This point is clearly well past the three-day minimum $E$ line and by interpolation it is easy to see that a minimum $E$ trajectory would take about 3.2 days to transfer to the same orbit. Now, while the minimum time trajectory has gotten to the same point in less time than the minimum $E$ trajectory, it has gone through more degrees of revolution to accomplish this. Thus the minimum time trajectory has gone through 37.69 radians of revolution; while, by interpolation, it can be seen that the minimum $E$ trajectory will reach the same point with only about 36.8 radians of revolution. In summary, a minimum time transfer takes 3.03 days in 37.69 radians, while the minimum $E$ transfer takes about 3.2 days in 36.8 radians.

Point L. Here the minimum $t$ trajectory has reached the point L

in 4.57 days while it takes the minimum E trajectory about 4.8 days. However, it takes the minimum t trajectory 50.26 radians of revolution as opposed to only about 47 radians of revolution for the minimum E trajectory.

Point P. This is a very good point for comparison. The minimum t flight time is 4.9 days. This is clearly less than the minimum E time, which is well past the five day line. The eccentric anomaly elapsed is 46.9 radians which clearly exceeds the value for the minimum E trajectory since point P is distinctly below the minimum E contour line where $E = 45.23$ radians.

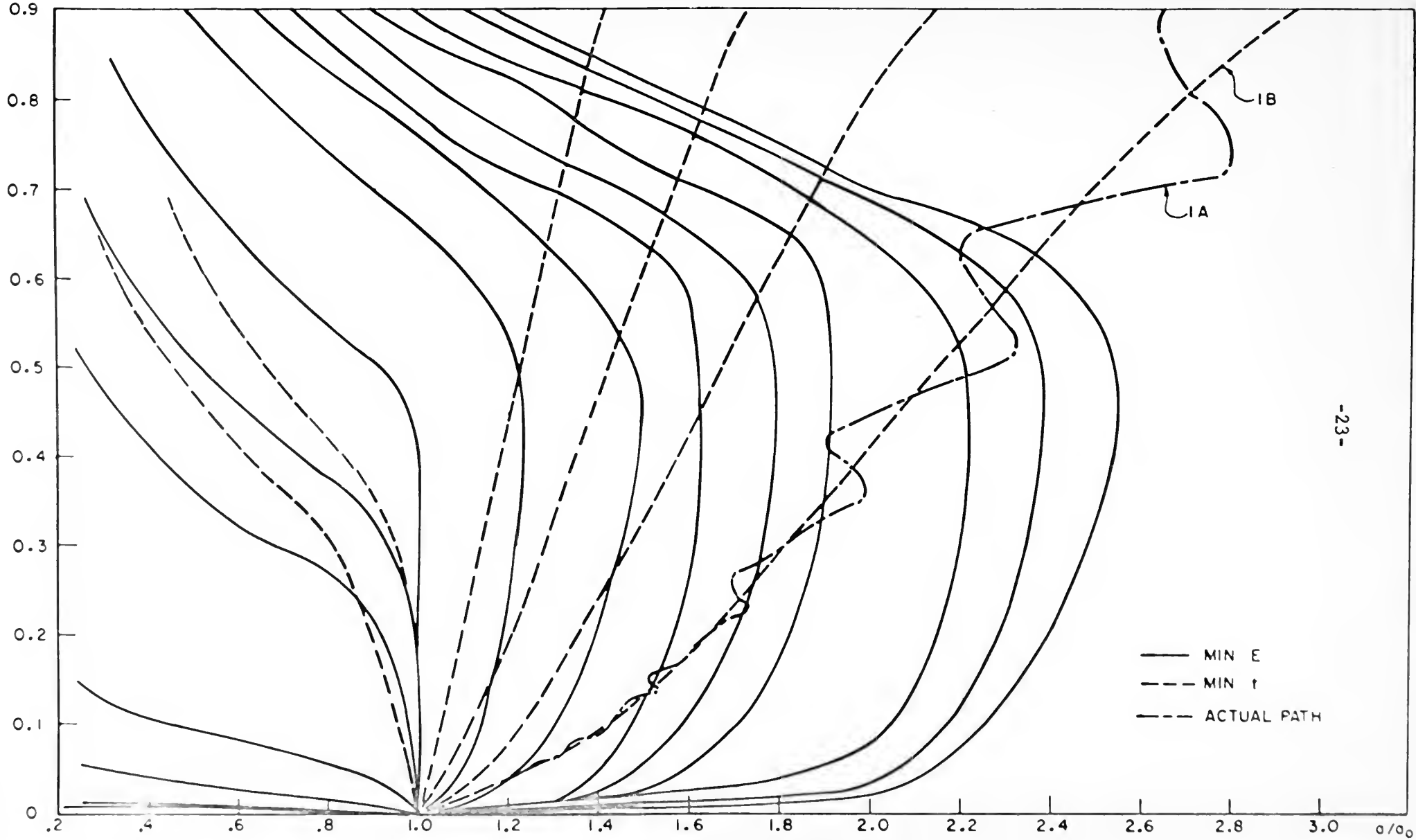


MINIMUM t AND MINIMUM E TRAJECTORIES
ON E VERSUS $A/A_0$ PLANE

FIGURE 3

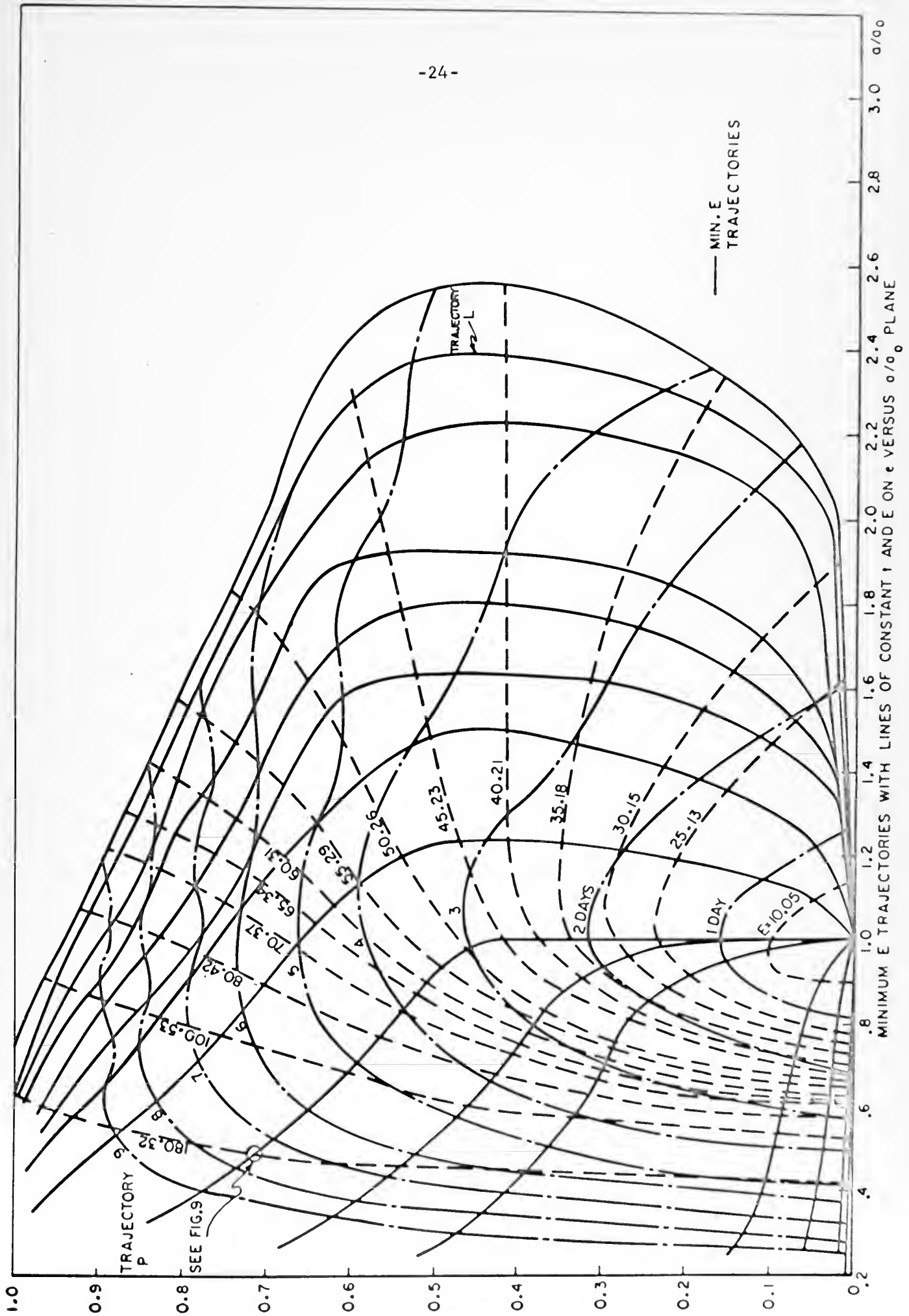
MINIMUM E TRAJECTORIES WITH LINES OF CONSTANT i AND E ON e VERSUS a/a0 PLANE
MIN. E TRAJECTORIES
TRAJECTORY L
TRAJECTORY P
SEE FIG.9
E=10.05
1 DAY
2 DAYS
25.13
30.15
35.18
40.21
45.23
50.26
55.29
60.31
65.34
70.37
80.42
105.53
80.32
a/a0
e

FIGURE 4

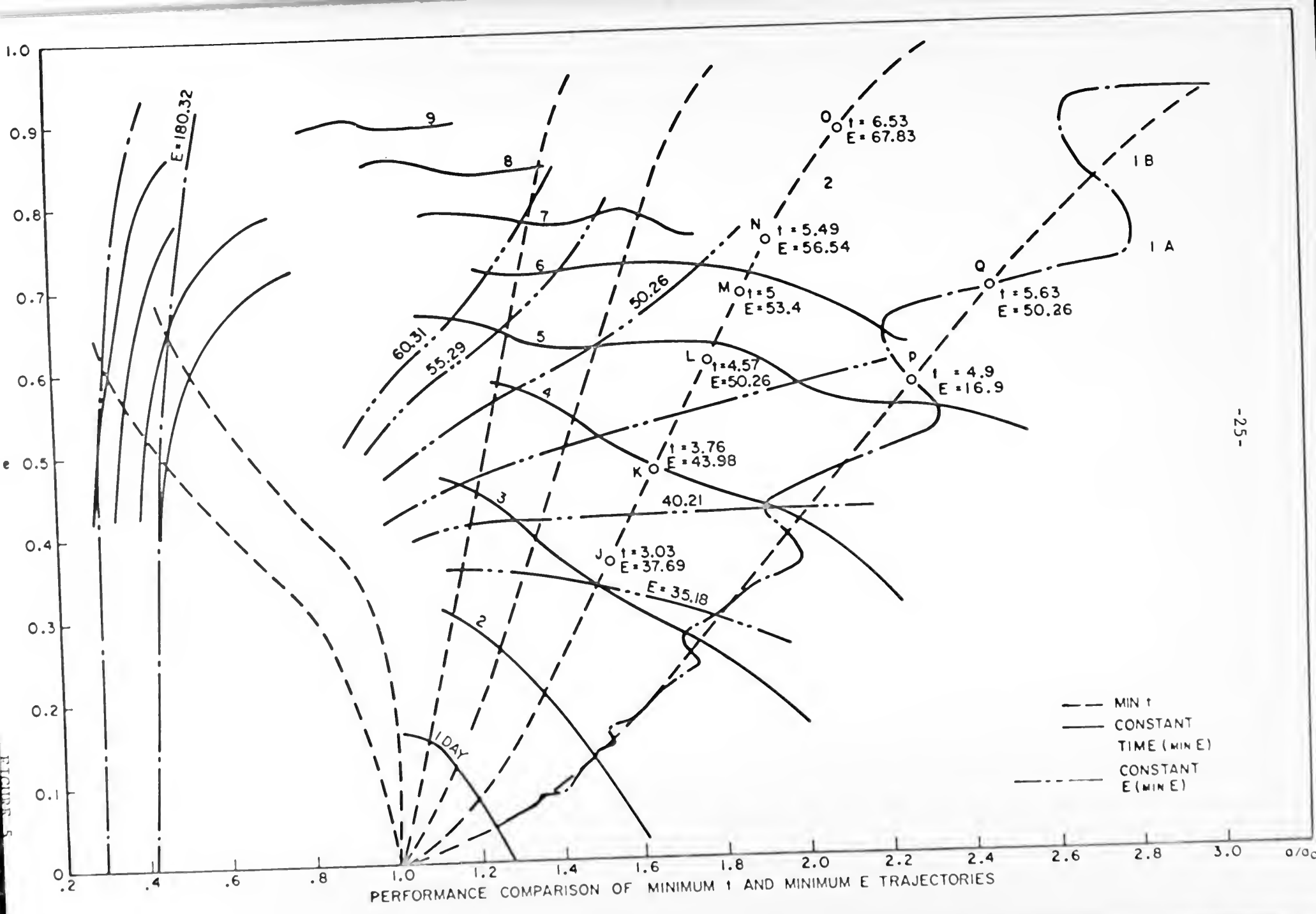


PERFORMANCE COMPARISON OF MINIMUM t AND MINIMUM E TRAJECTORIES

FIGURE 5

## VII. DISCUSSION OF OSCILLATORY MOTION

### A. Effect of Thrust Acceleration and Lagrangian Multipliers on Oscillatory Motion

Through numerous computer runs, it was verified that different thrust accelerations produce essentially the same mean transfer trajectories, providing the Lagrangian multipliers are scaled according to the ratio of the accelerations (observe Figure 6). A very low thrust system produces a trajectory with minimal oscillatory motion (curve $A_2$). As the thrust acceleration is increased, and the Lagrangian multipliers scaled accordingly, the oscillatory motion of the transfer trajectory becomes much more pronounced (curve $A_1$), while the mean trajectory remains the same as with the lower thrust acceleration.

It has also been verified (Figure 7) that minute changes in the initial Lagrangian multipliers result in uniquely different transfer trajectories which do not overlap, as long as the same thrust acceleration is used. The transfer trajectories can overlap if both the Lagrangian multipliers and the thrust acceleration are changed (Figure 8).

Figure 9 shows orthogonality between minimum E trajectories and constant E path which must exist for optimal solutions. This is a good check on the problem solution. In this case, each point was plotted to show the detailed angular orientation of the two curves at the point of intersection. The smoothed-in path of trajectory P in Figure 4 does not appear to show orthogonality, but close observation, i.e., blow-up in Figure 9, proves it to be so.

### B. Appearance of Negative Eccentricities

An interesting and perplexing problem was encountered while examining

the oscillatory points along trajectories at very small eccentricities. The problem is one which involves explaining the presence of a few negative eccentricity values which appear during the calculation of transfers of low eccentricity. Figures 10 and 11 illustrate this point. In the blow-up of area I in Figure 11, points A, B, C and D all lie below the axis and are thus negative eccentricities (of very low magnitude) and are printed out as such by the computer.

These negative points appear to be in line with the normal cycle of the oscillatory motion. Another point to note is that none of the smoothed trajectories ever go below zero eccentricity; that is to say, at the end of every cycle (i.e., for every $2n\pi$ of eccentric anomaly) $e$ is always greater than or equal to zero. However, to date there is no clear meaning accorded to these negative eccentricities. Further analysis is necessary to determine the real significance of this factor.

C. Oscillatory Motion and the $\xi$ Function

Also connected with the oscillatory motion which accompanies all spiral trajectories is the $\xi$ function as defined in equation (40). Through many minimum $t$ program runs, it was found that the $\xi$ function never stays at zero but always oscillates through zero once every revolution, usually at every $2n\pi$ of eccentric anomaly. The smoothed $\xi$ function is zero, but the minimum $t$ formulation states that the $\xi$ function must equal zero at the terminal point in order to represent an optimal transfer. Therefore, the transfers are exactly optimal once every revolution when the $\xi$ function is zero and are near optimal in between. The minimum $E$ transfers are exactly optimal at all points along the trajectory since there is no $\xi$ function requirement in that formulation.

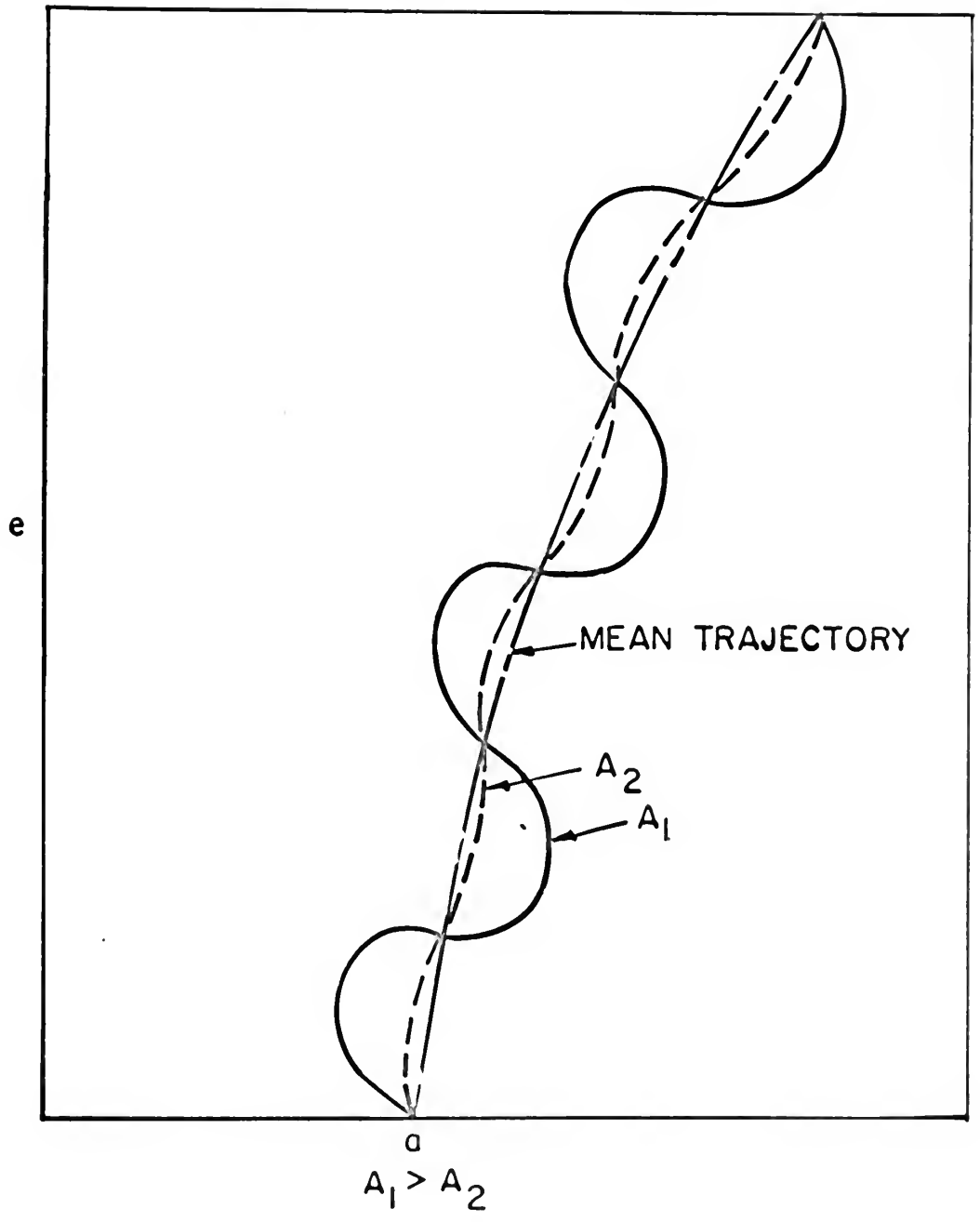


COMPARISION OF TRAJECTORY OSCILLATORY MOTION FOR DIFFERENT VALUES OF THRUST ACCELERATION

FIGURE 6

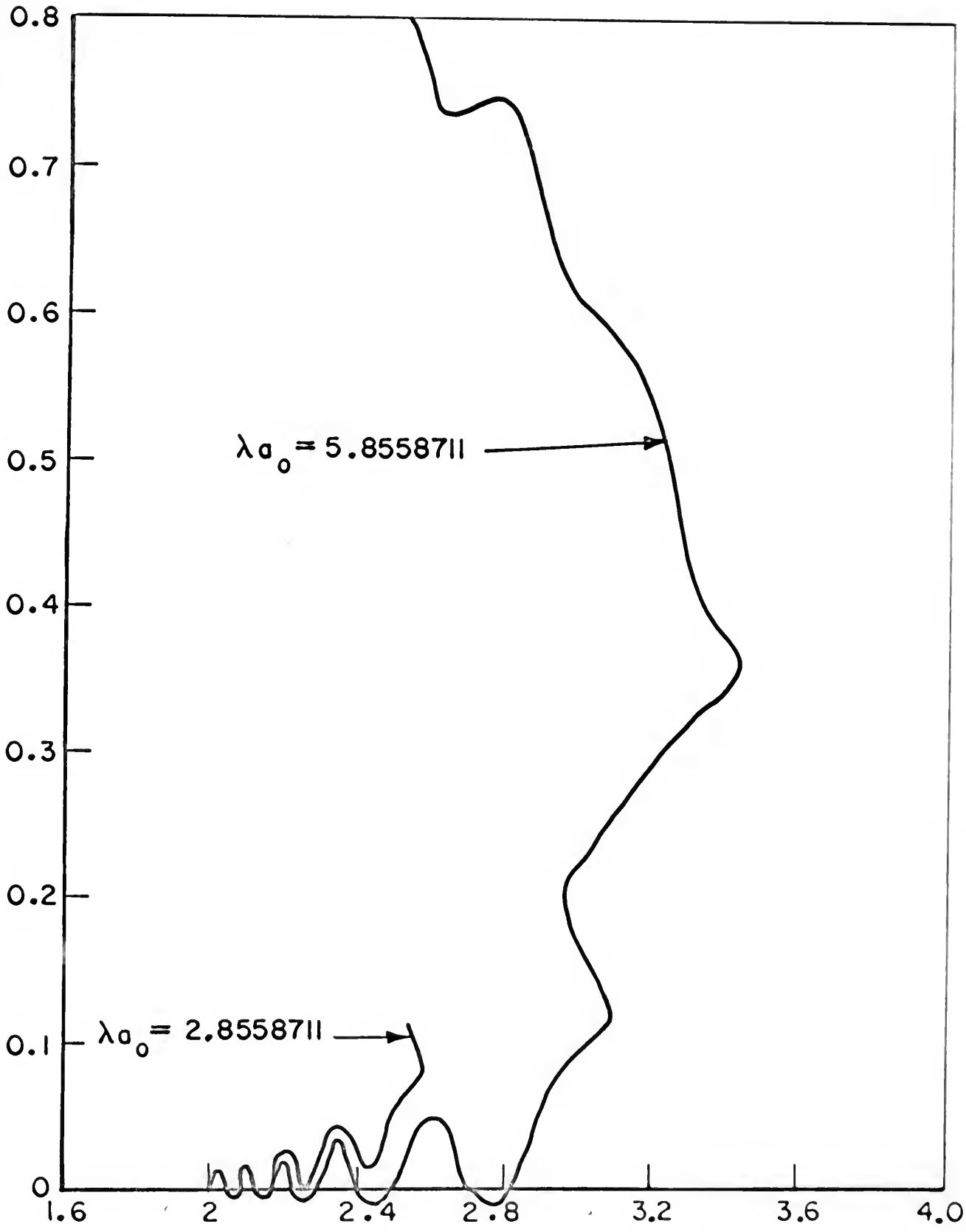


COMPARISON OF TRAJECTORY OSCILLATORY MOTION
FOR DIFFERENT VALUES OF LAGRANGIAN MULTIPLIERS

FIGURE 7

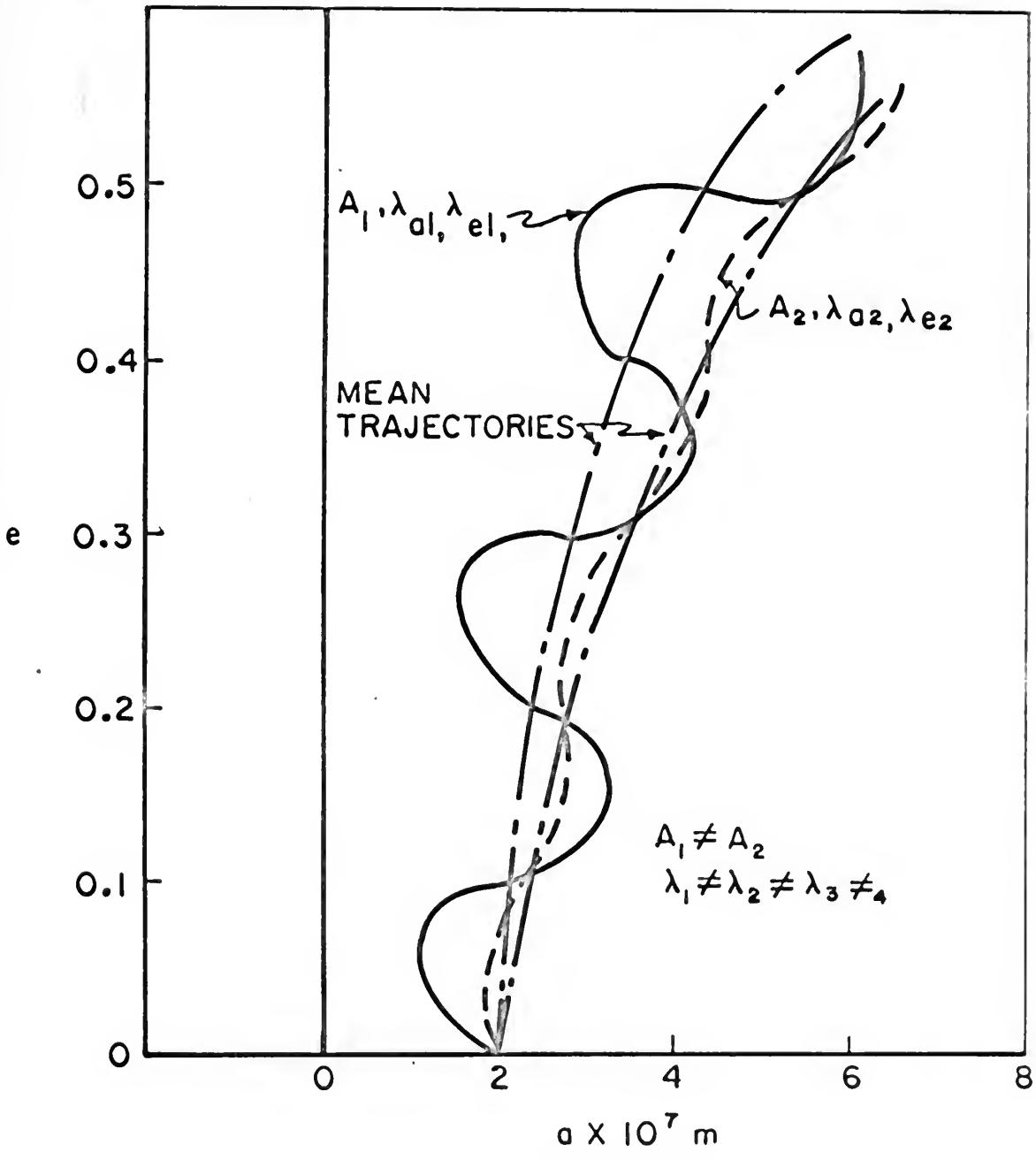


COMPARISON OF TRAJECTORIES FOR DIFFERENT VALUES OF THRUST ACCELERATION AND LAGRANGIAN MULTIPLIERS

FIGURE 8

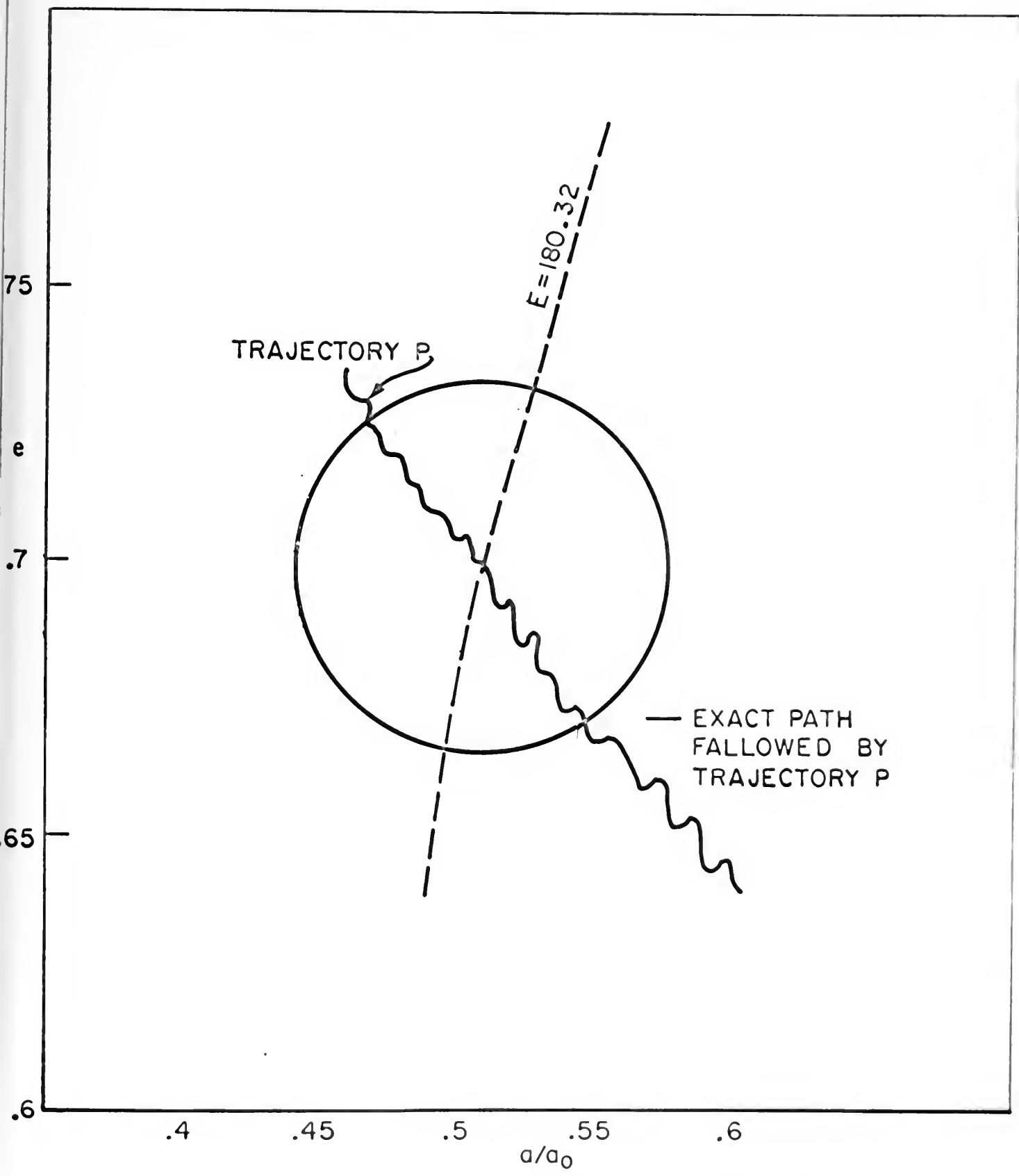


BLOW—UP OF MINIMUM E TRAJECTORY P SHOWING ORTHOGONALITY BETWEEN THE TRAJECTORY AND THE CONSTANT E PATH WHICH MUST EXIST FOR OPTIMAL SOLUTIONS.

FIGURE 9

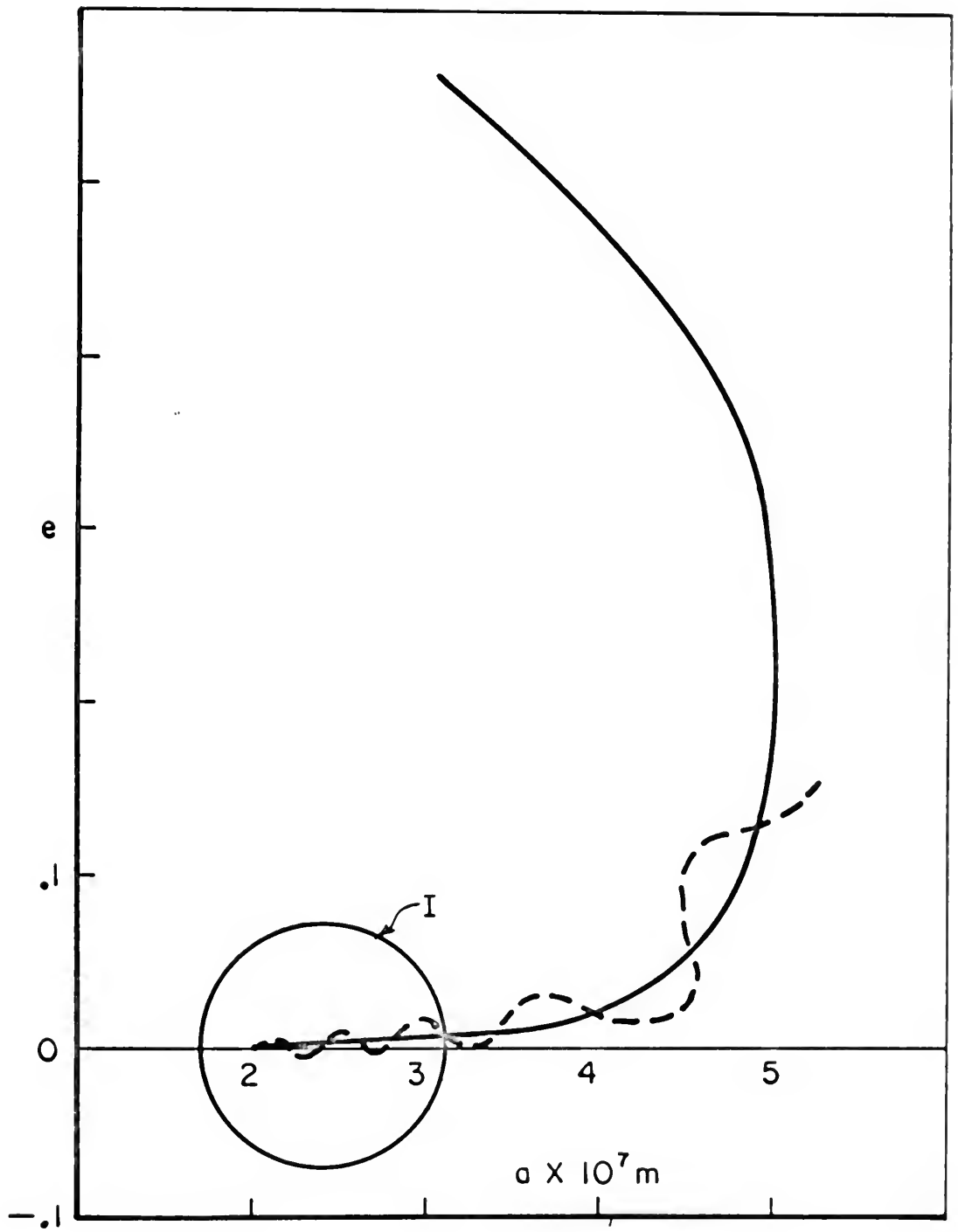


OCCURENCE OF NEGATIVE ECCENTRICITIES

FIGURE 10

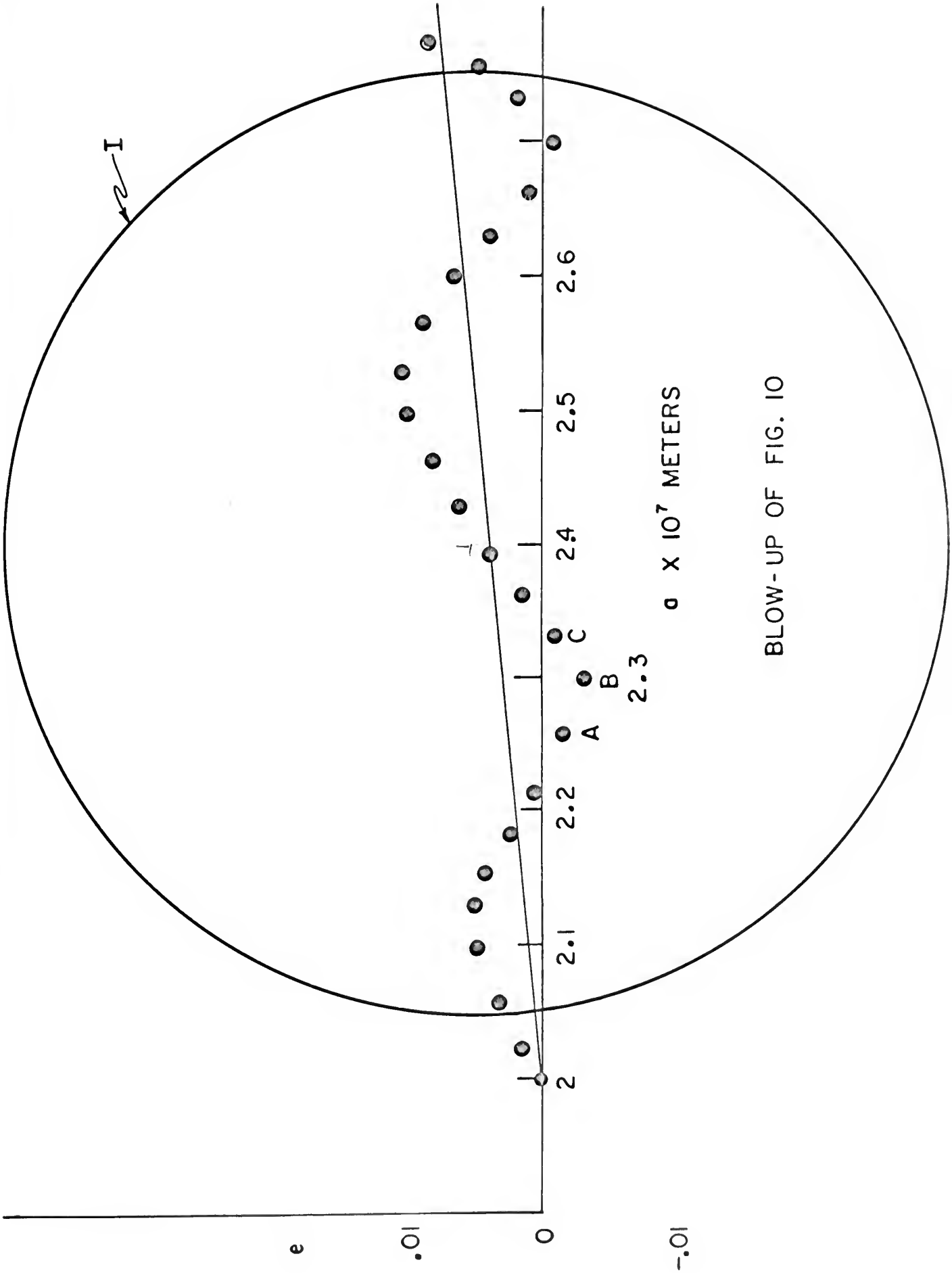


FIGURE 11

## VIII. COMPUTATIONAL COMPARISON WITH EDELBAUM'S VARIABLE THRUST CALCULATIONS

### A. Examining Thrust Angle Schemes for Different Trajectories

An optimal variable thrust system can be utilized to measure the limit of best possible performance with an optimal fixed-thrust system. This is so because of the extra degree of freedom added to the control system when the variable thrust is incorporated, making it a more efficient system than the fixed-thrust one. Thus, any optimal performance by the fixed-thrust system can, at best, be only equal to the optimal variable thrust system and, more often than not, it will be less than the variable thrust system's performance.

The following equations were derived by Edelbaum (References 1, 2, 3) for optimal variable thrust trajectories using an averaging technique and are used here for comparison with the fixed-thrust performance:

$$V_c^2 = 2J\, t_f = \overline{A^2}\, t_f^2 = \frac{k}{a_o}\left[1 + \frac{a_o}{a} - 2\sqrt{\frac{a_o}{a}}\cos\left(\sqrt{\frac{2}{5}}\left\{\sin^{-1} e - \sin^{-1} e_o\right\}\right)\right] \tag{81}$$

$$(\Delta V_c)^2 \equiv \overline{A^2}\, T^2 = \frac{k}{a_o}\left[\left(\frac{\Delta a}{2a}\right)^2 + \frac{2}{5}\,\frac{(\Delta e)^2}{1-e^2}\right] \tag{82}$$

$\overline{A^2} \equiv$ the averaged squared variable thrust acceleration over a turn = a constant (83)

$$J \equiv \int_o^{t_f} \frac{A^2}{2}\, dt = \frac{\overline{A^2}}{2}\, t_f \tag{84}$$

$$\frac{1}{m_f} = \frac{1}{m_o} + \frac{J}{P} \tag{85a}$$

$$P = \text{POWER} = \frac{1}{2} \left| \dot{m} \right| v_j^2 \tag{85b}$$

Equation (81) applies to large changes in (a, e); i.e., more than one revolution. Equation (82) is a special case of (81) and applies only to changes within one turn.

To compare the two propulsion systems, $V_c$ and $\Delta V_c$ for fixed thrust are both defined as:

$$V_c = \Delta V_c = A \times t \ (\Delta t) \tag{86}$$

As can be seen in Table 1, the fixed thrust $V_c$ and $\Delta V_c$ are always larger than the corresponding variable thrust $V_c$ or $\Delta V_c$ where:

$$C_1 \equiv \frac{(\Delta V) \text{ fixed}}{(\Delta V) \text{ variable}} \tag{87}$$

Note that $C_1$ is always greater than 1. This indicates a higher cost for the fixed thrust system as expected.

As might be anticipated in cases involving near-circular orbits the thrust magnitude of the variable thruster is almost constant, yielding the same case as the fixed thrust system. Here the value for $C_1$ is very close to one. When transfers are conducted with more elliptical orbits, the variable thrust system thrust magnitude scheme no longer resembles the fixed thrust case, and the cost is then less, making $C_1$ take on larger values.

B. Maximum $\Delta a$ and $\Delta e$ Steering Programs

It is interesting and instructive to see how the thrust angle varies throughout each transfer. Though only the angle varies (and not the magnitude of the thrust) in fixed thrust transfers the angle program agrees closely to the one calculated by Edelbaum (See Figure 12). The thrust at points A through E coincide in both direction and magnitude.

Examining single turn characteristics, if $e$ is changing more rapidly than $a$, then the second term on the right-hand side of equation (82) will dominate the first term. Similarly, if $a$ is changing more rapidly than $e$, then the first term dominates the second term. Figure 12 shows the thrust schemes for maximum $\Delta a/a$ and maximum $\Delta e$ programs. The last two columns in Table 1 show that when the predominant change is in $a$, then the thrust scheme is an "a" thrust scheme and vice versa.

The fact that Table 1 indicates close but slightly inferior performance for the fixed thrust when compared with the variable thrust lends considerable support to the validity of both sets of calculations.

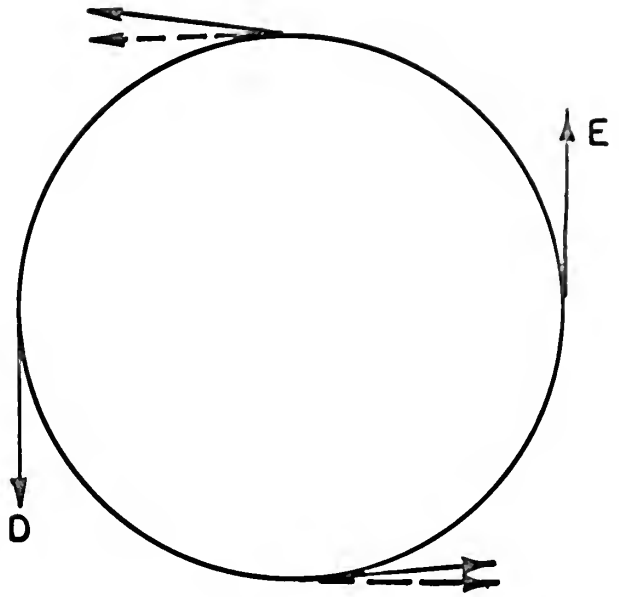


MAXIMUM Δ a

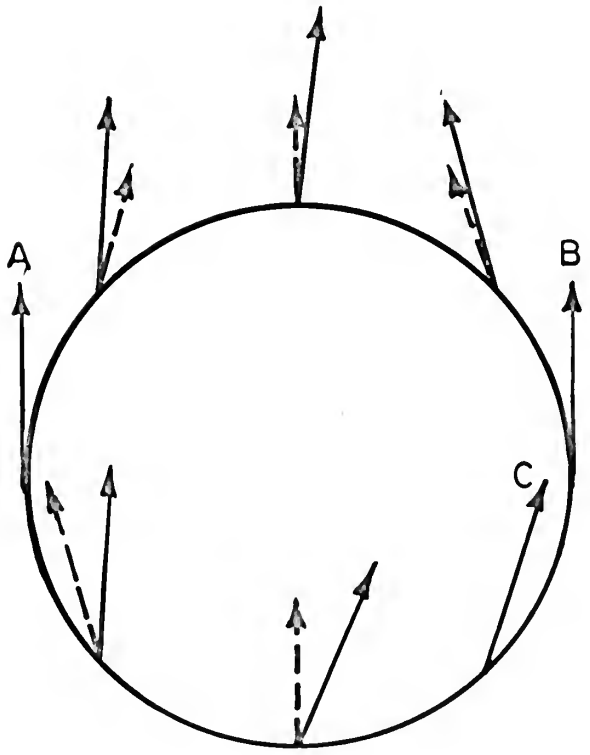


MAXIMUM Δ e

——— FIXED

– – – VARIABLE

COMPARISON OF FIXED THRUST WITH VARIABLE THRUST FOR TRANSFERS WHICH START WITH CIRCULAR ORBITS

Table 1

Comparison of Fixed-Thrust Acceleration with Variable-Thrust Acceleration Performance

Constants: $A = 5\times10^{-3}$ m/s$^2$ $\quad k = 3.22\times10^{14}$ m$^3$/s$^2$ $\quad \lambda_{e_o} = 2.054691\times10^{5}$ $\quad \lambda_{a_o} = 1.171174\times10^{-2}$

$C_1 \equiv (\Delta V)$ actual $/$ $(\Delta V)$ variable $\qquad C_2 \equiv \left(\frac{0.4\ (\Delta e)^2}{1 - e_o^2}\right) \Big/ \left(\Delta a / 2a_o\right)^2$

| Turn Nos. | $E_o$ (rad.) | $t_o$ (days) | E (rad.) | t (days) | $e_o$ | $a_o$ mx$10^7$ | $e_f$ | $a_f$ mx$10^7$ | Actual V m/s | $C_1$ | $C_2$ | Predominant change | Steering Program Type |
|---|---|---|---|---|---|---|---|---|---|---|---|---|---|
| 1st | 0 | 0 | 2 | .3823 | 0 | 1.9975 | .01541 | 2.1536 | 165 | 1.015 | .062 | | |
| 5th | 8 | 1.8923 | 2 | .6852 | 1.1005 | 2.895 | .1889 | 3.2469 | 296.1 | 1.123 | .68 | a | a |
| 9th | 16 | 5.632 | 2 | 1.639 | .679 | 4.946 | .9112 | 6.082 | 710 | 1.176 | 3.31 | e | e |
| 0 to 9 | 0 | 0 | 18 | 7.271 | 0 | 1.9975 | .9112 | 6.082 | 3121 | 1.120 | - | - | - |
| | | | | $\lambda_{e_o} = 3.031434\times10^{5}$ | | $\lambda_{a_o} = 1.711742\times10^{-2}$ | | | | | | | |
| 1st | 0 | 0 | 2 | .3818 | 0 | 1.9975 | .0174 | 2.149 | 164.9 | 1.033 | .0843 | a | a |
| 6th | 10 | 2.389 | 2 | .649 | .2482 | 2.848 | .3484 | 3.060 | 280 | 1.11 | 3.12 | e | e |
| 11th | 20 | 6.536 | 2 | 1.216 | .8734 | 4.237 | .9758 | 4.7029 | 525 | 1.42 | 58.7 | e | e |
| 0 to 11 | 0 | 0 | 22 | 7.752 | 0 | 1.9975 | .9758 | 4.7029 | 3355 | 1.11 | - | - | - |
| | | | | $\lambda_{e_o} = 4.762868\times10^{5}$ | | $\lambda_{a_o} = -1.166968\times10^{-2}$ | | | | | | | |
| 1st | 0 | 0 | 2 | .3561 | 0 | 1.9975 | .05271 | 1.9519 | 154 | 1.082 | 8.55 | e | e |
| 8th | 14 | 2.497 | 2 | .253 | .3107 | 1.601 | .3283 | 1.541 | 109 | 1.112 | .39 | a | a |
| 75th | 148 | 9.756 | 2 | .061 | .6428 | .613 | .6451 | .6091 | 26.45 | 1.0095 | .341 | a | a |
| 0 to 75 | 0 | 0 | 150 | 9.817 | 0 | 1.9975 | .6451 | .6091 | 4240 | 1.036 | - | - | - |

Per turn $\quad (\Delta V)_{\text{variable thrust}} = \sqrt{\frac{k}{a_o}} \left[\left(\frac{\Delta a}{2a_o}\right)^2 + .4\ \frac{(\Delta e)^2}{1-e_o^2}\right]^{\frac{1}{2}}$

Many turns $\quad (\Delta V)_{\text{variable thrust}} = \sqrt{\frac{k}{a_o}} \left\{1 + \frac{a_o}{a_f} - 2\sqrt{\frac{a_o}{a_f}}\ \cos\left[\sqrt{.4}\ \left\{\sin^{-1}e_f - \sin^{-1}e_o\right\}\right]\right\}^{\frac{1}{2}}$

## IX. DETAILED ANALYSIS OF THE THRUST ANGLE SCHEME FOR A MINIMUM E TRAJECTORY

The minimum E trajectory L from Figure 4 was selected for examination of its thrust angle scheme. The optimal, computed thrust angle was recorded and plotted versus eccentric anomaly (see Figure 13). The trust angle positions were recorded every 90 degrees of eccentric anomaly for every third revolution.

Figure 4 shows that for the first 2.6 days the thrust program changed primarily the semi-major axis. In this time period a doubled from 2 to $4 \times 10^7$ meters while the eccentricity increased very slowly from 0 to about 0.03. This part of the transfer is depicted in Figure 14 where the original orbit is $0_1$, and after 2.6 days the trajectory has reached orbit $0_2$. Thus the program starts out by increasing the semi-major axis with little change in eccentricity; it uses essentially a maximum $\Delta a$ thrust angle scheme with mostly tangential thrust. This can be seen by observing the thrust angle scheme for revolutions one and four in Figure 13.

By observing trajectory L in Figure 4 one can see that between $t = 2.6$ and $t =$ about 4.6 (days) the thrust program changes to a maximum $\Delta e$ trajectory, while remaining fairly static in its semi-major axis. Figure 15 depicts this leg of the transfer from orbit $0_2$ to orbit $0_3$. These orbits were chosen at appropriate points to illustrate the computed trajectory. A drastic change in the thrust angle scheme between revolutions four and seven can be seen in Figure 13.

Figure 16 shows the transfer between $t = 4.6$ and $t =$ about 11 days.

The semi-major axis $a$ decreases steadily while $e$ increases. The engine is cut off when the trajectory reaches orbit $0_4$. At this point $e = 0.998$ and $a = 1.24 \times 10^7$ meters. It is interesting to note that between $t = 4.6$ and 11 days, as the program begins to change $a$ more rapidly, the thrust angle pattern (between revolutions 10 and 27) begins to revert back again toward a tangential type thrust scheme (Figure 13).

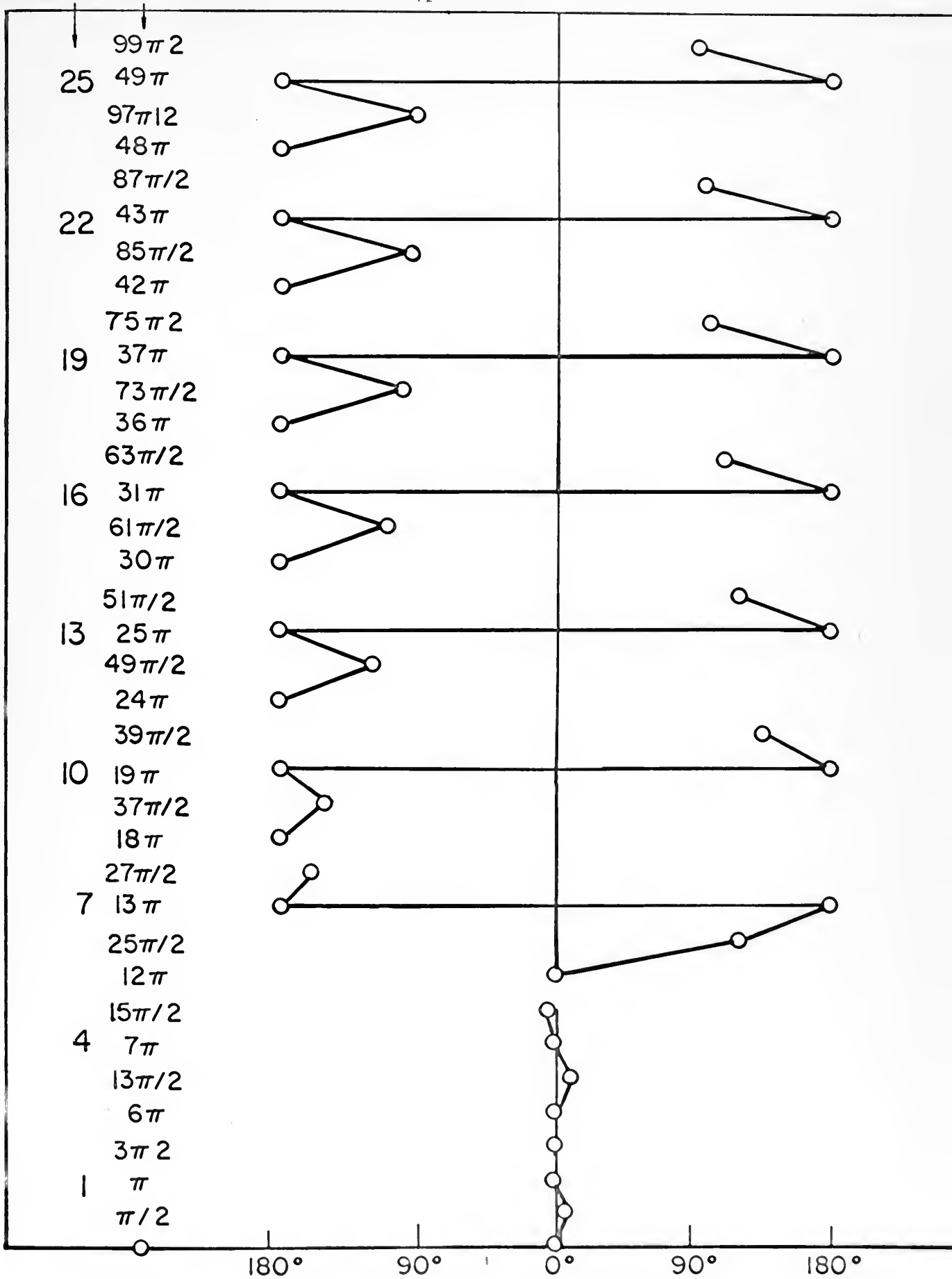


THRUST ANGLE SCHEME FOR MINIMUM E TRAJECTORY L

FIGURE 13

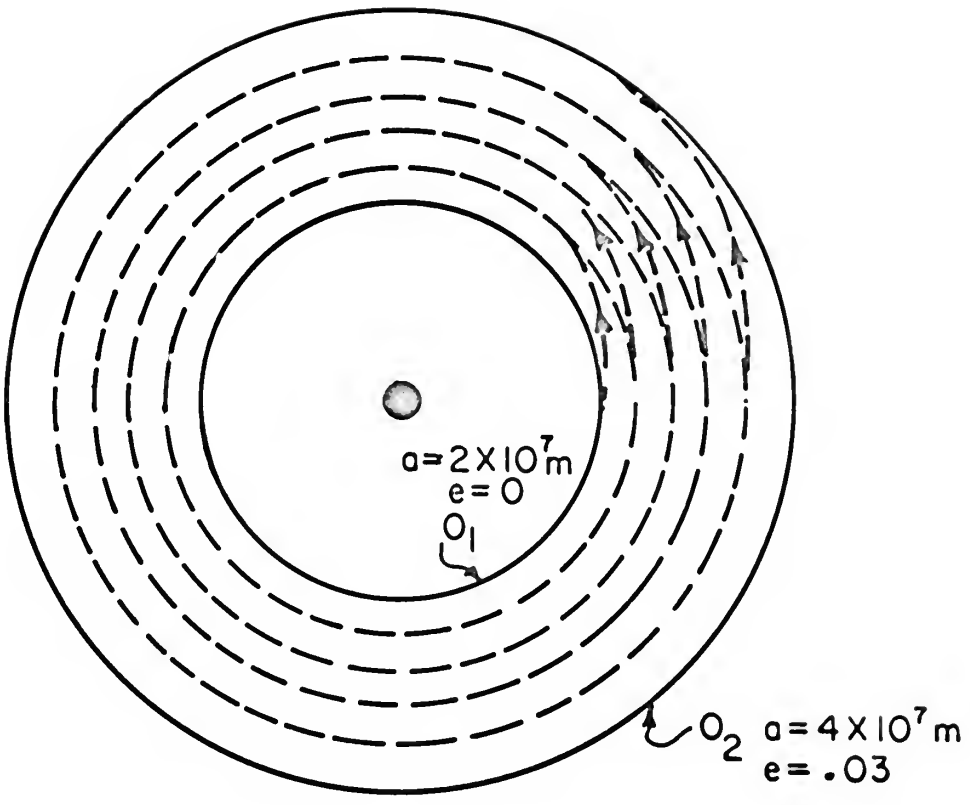


STARTING FROM ORBIT $O_1$ THE SPIRALING PROCESS HAS REACHED ORBIT $O_2$ AT t = 2.6 DAYS.

FIRST LEG OF MINIMUM E TRAJECTORY L SHOWING MAXIMUM $\Delta a$ STEERING SCHEME

FIGURE 14

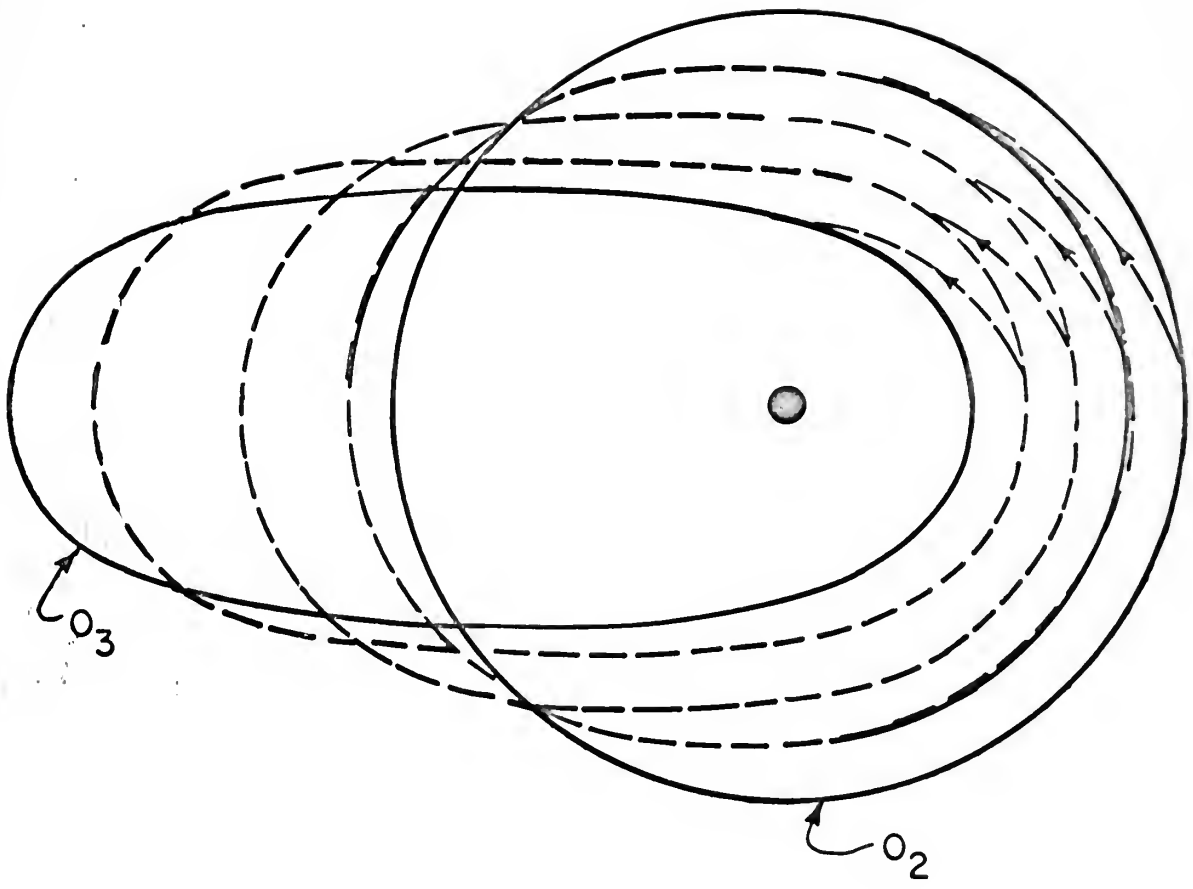


AT $t = 4.6$ DAYS THE ORBIT SPIRALING PROCESS HAS CARRIED THE VEHICLE TO $O_3$.

SECOND LEG OF MINIMUM E TRAYECTORY L SHOWING MAXIMUM $\Delta e$ STEERING SCHEME

FIGURE 15

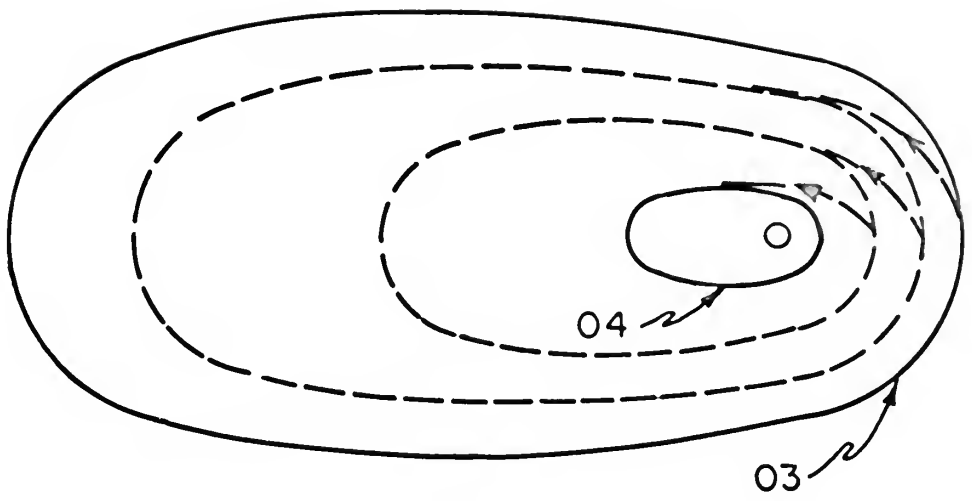


AT t = 11 DAYS, THE VEHICLE HAS BEEN TRANSFERRED TO ORBIT $O_4$ AT THIS POINT THE ENGINE IS CUT OFF AND THE VEHICLE REMAINS IN THE SPECIFIED ORBIT $O_4$.

FINAL STAGE OF MINIMUM E TRAJECTORY L SHOWING ATTAINMENT OF DESIRED FINAL ORBIT ($O_4$)

FIGURE 16

# X. MARS ORBITAL TRANSFER

## A. Description of Problem

In order to gain a practical comparison with single impulse chemical retro transfers, realistic values were assigned to solar electric and chemical rocket engines to be used in an orbital transfer about the planet Mars. An initial elliptical orbit was chosen with large eccentricity and large semi-major axis (when compared to the radius of Mars). The problem involved transferring from this initial orbit into a much smaller circular orbit with radius of 1.1 that of the radius of Mars. The periapse of the initial elliptical orbit is equal to the radius of the desired final circular orbit.

The low-thrust spiral transfer is accomplished by turning on the solar electric engine at the initial ellipse periapse, causing the space vehicle to slowly spiral into the desired final circular orbit using the optimized thrust angle program for fixed thrust. The retro transfer is accomplished by using a single chemical rocket retro at the ellipse periapse causing the space vehicle to transfer directly into the circular orbit. The amount of fuel required for each transfer is then compared. The purpose of the spiral transfer is to deliver a larger payload to the final orbit. One must then decide if the increase in payload delivered is worth the extra time required to make the transfer. Figure 17 shows the two methods of transfer being compared, the upper drawing being the spiral transfer and the lower one depicts the single chemical retro impulse transfer at the ellipse periapse.

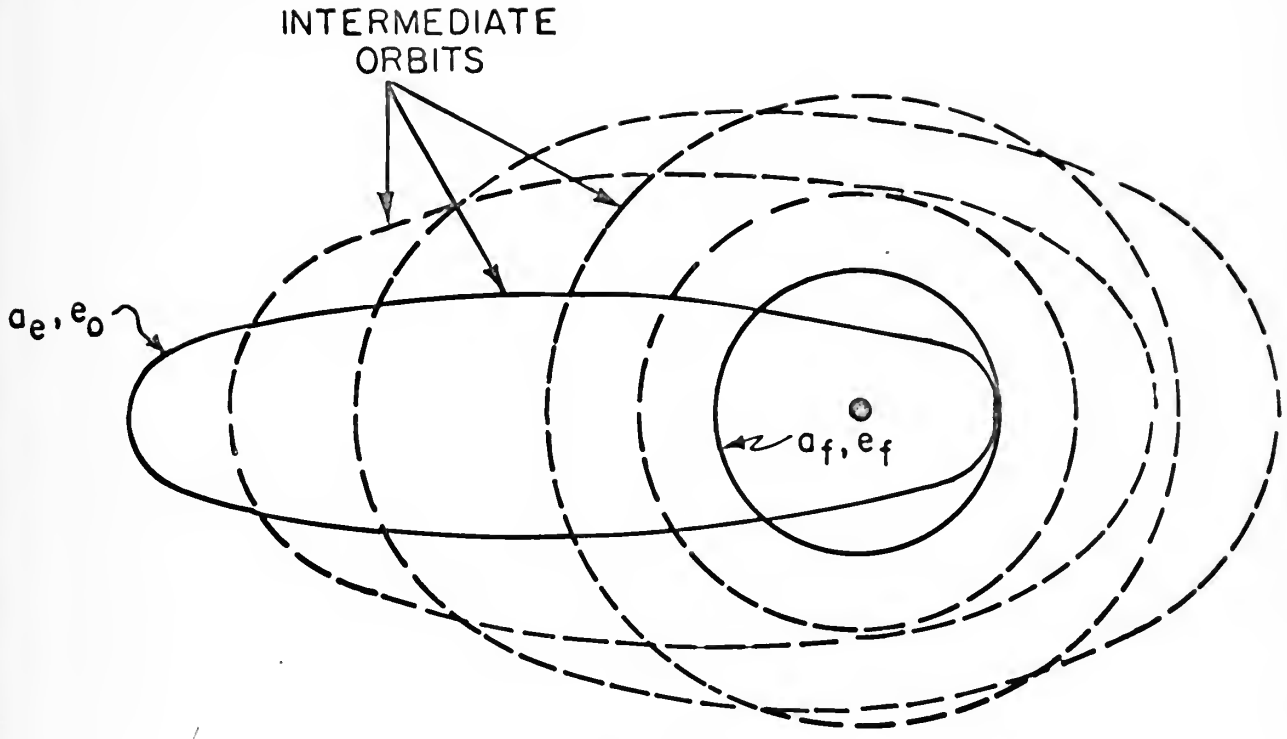


SPIRAL TRANSFER

$a_o = 9.734764 \times 10^7$ METERS

$e_o = 0.95773909$

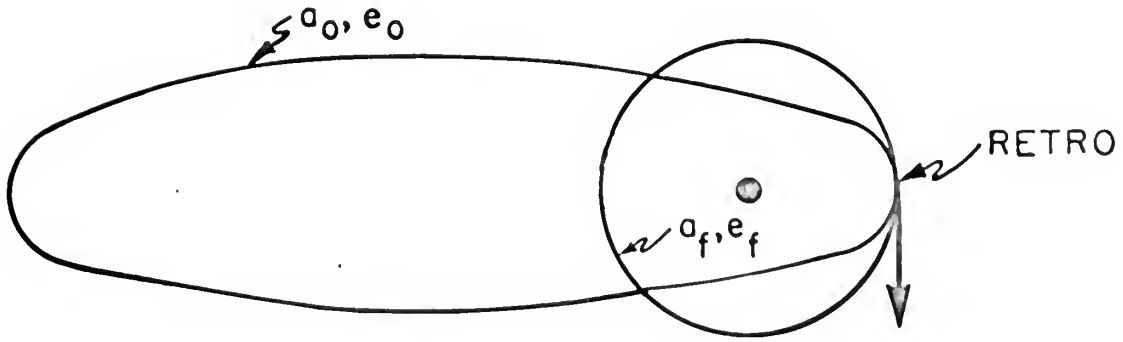


CHEMICAL ROCKET RETRO

MARS ORBITAL TRANSFER

FIGURE 17

B. Initial Data Used

The values used in this comparison were as follows (Reference 8):

Solar Electric Engine

$$F = 0.59756046 \frac{kg \cdot m}{s^2}$$

$$v_j = 39,464.9 \text{ m/s}$$

Chemical Rocket Engine

$$v_j = 2890.49 \text{ m/s}$$

Both Engines

$$M_{ell} = \text{initial mass in ellipse} = 2049.5093 \text{ kg}$$

radius of Mars: 3400 km

$$k_{Mars} = 4.293 \times 10^{13} \text{ m}^3/\text{s}^2$$

$$a_{ell} = 9.734764 \times 10^{7} \text{ m}$$

$$e = 1 - \frac{r_{e_p}}{a_{ell}} = 0.95773909$$

C. Chemical Rocket Transfer

The Mathematical Development follows:

$$v_{e_p} = \text{velocity at ellipse periapse}$$

$$= \sqrt{\frac{2k}{r_{e_p}} - \frac{k}{a}} \qquad (88)$$

$$= 4.6389 \times 10^{3} \text{ m/s}$$

$$v_c = \text{velocity at final circular orbit}$$

$$= \sqrt{\frac{k}{a}} = 3,390 \text{ m/s}$$

$$\Delta v_c = v_{ep} - v_c = 1,248.9 \text{ m/s} \qquad (89)$$

$m_{c_1}$ = mass in final circular orbit after chemical retro

$$m_{c_1}/m_{ell} = e^{-\Delta v/v_j} = e^{-1248.9/2890.49} \tag{90}$$

$$= e^{-.431} = .652$$

So $m_{c_1} = (.652)(2049.5093) = 1{,}340$ kgs

$$\therefore \quad \Delta m_{c_1} = \begin{array}{r} 2049.5093 \\ -1340.0000 \\ \hline 709.5093 \text{ kgs} \end{array}$$

Thus, the direct chemical rocket insertion requires 709.5093 kg of fuel with an initial total vehicle mass of 2049.5093 kg. This means that a total mass of 1,340 kg is delivered into final orbit by this method.

D. Optimized Fixed-Thrust Acceleration Spiral Transfer

Next, the same transfer is accomplished using the solar electric spiral technique. Assuming the same initial ellipse and total vehicle mass, the initial thrust acceleration is determined:

$$A = \frac{F}{m_{ell}} = 2.92\text{x}10^{-4} \text{ m/s}^2$$

Although assumed a constant, A will actually increase as the vehicle mass decreases due to loss of fuel. A mean value of about $3\text{x}10^{-4}$ $m/s^2$ was used in the programs, which implies a total anticipated change of about 6 percent in thrust acceleration. The time to spiral optimally to $e_f$, $a_f$ was computed to be 128.685 days. To compute the fuel expended while spiraling into the final circular orbit (Reference 9):

$$F = \left|\dot{m}\right| v_j \tag{91}$$

$$\left|\dot{m}\right| = \frac{F}{v_j} = \frac{.59756046 \text{ kg.m/s}^2}{39{,}464.9 \text{ m/s}}$$

$$\dot{m} = 1.515\text{x}10^{-5} \text{ kg/s}$$

To find the fuel expended while spiraling, $\Delta m_s$, multiple $|\dot{m}|$ by the total time t elapsed during the spiraling process:

$$\Delta m_s = |\dot{m}| t \tag{92}$$

Now,

$$t = 128.685 = 1.11716 \times 10^7 \text{ sec}$$

$$\Delta m_s = (1.515 \times 10^{-5} \text{ kg/s})(1.11716 \times 10^7 \text{ s})$$

$$= 169 \text{ kg}^*$$

E. Results and Comparison of Data

Thus, the solar electric spiraling process has accomplished the same transfer while using only 169 kg of fuel. This yields

| | |
|---|---|
| Initial mass | 2049.5093 |
| Fuel | - 169.0000 |
| $m_{c_2}$ | 1880.5093 kg |

1880.5093 kg of mass is delivered into final circular orbit by the solar electric method. Since 709.5093 kg of fuel were required by the chemical retro transfer, and only 169 kg were expended during the solar electric spiral, the latter method yields a savings of 540.5093 kg or about 1150 pounds.

These results mean that the desired final circular orbit can be obtained almost instantaneously by chemical insertion, but with a cost of 709.5093 kg of fuel; or, the same orbital transfer can be accomplished over a period of 128.685 days with a cost of only 169 kg of fuel. Thus, if one chose the slower spiral technique, the amount of payload delivered to final orbit could be increased by about 1150 pounds. The advantages and disadvantages of

---

*Note that for constant thrust magnitude, the total increase in thrust acceleration due to fuel depletion = 9 percent.

each method must be weighed along with the mission objectives to arrive at a decision over which method should be used. It would seem that the spiral technique as described would be far better suited to an unmanned observational missions than the chemical method (Reference 10). It would seem impractical to use the slow spiral technique on any manned flights, regardless of the fuel saved, but this does not preclude the use of solar electric engines enroute to various destinations as a thruster boost.

## XI. CONCLUSIONS AND RECOMMENDATIONS

The numerical solution of the optimum fixed-thrust acceleration elliptic spiral technique has been used to generate many different planeto-centric transfer trajectories. Figure 2 represents an infinite number of minimum time and minimum eccentric anomaly transfers. It should be noted that any transfer generated can also be reversed by appropriate manipulation of the Lagrangian multipliers. Optimized transfers can be conducted from any point along a generated trajectory to another point on that trajectory. This is done by starting the program with the Lagrangian multipliers already printed out at the desired point along the trajectory.

At present there is no analytic method for choosing the Lagrangian multipliers for particular transfers. By generating many transfer trajectories, one can accumulate many cases, but the initial process involved in choosing the Lagrangian multipliers remains guesswork and experimentation. Possibly by examining more closely the transfers produced by the numerical solutions used herein one might draw some clues for the analytic solution. The use of reiteration techniques to converge initial guesses to final correct values was not explored in this thesis, but is a well-established art (Reference 11).

As mentioned in an earlier section, all transfers were designed to be coplanar, and co-axial. As expected, virtually no rotation of the line of apsides was observed. A problem noted and recommended for further study was the occasional production of very small negative eccentricities along certain transfer trajectories. It only occurs in transfers involving circular or near-circular orbits and then only in transfers displaying maximum $\Delta\alpha$ thrust

angle schemes.

The hypothetical Mars orbital transfer conducted under realistic conditions yields some interesting facts for consideration. The optimized spiral technique proves to be able to deliver up to 1150 pounds more into the desired final orbit than the single impulse chemical retro method, based upon a decrease in the amount of fuel required to accomplish the transfer. However, the spiral transfer requires 128 days to make the transfer, while the chemical method works almost instantaneously.

Another possibility would be to assume that no more payload is required on this particular flight, in which case the extra 1150 pounds could be trimmed from the initial mission weight. This would greatly reduce the fuel required to launch the vehicle from earth orbit; or, one could use the same amount of booster fuel in which case the vehicle would reach the target planet much faster than before and would thereby decrease the overall flight time. One must then look at all of the factors involved in particular missions to determine which method or combination of methods might be most useful.

While this thesis has addressed itself only to the use of optimized fixed-thrust orbital transfers, it is quite conceivable, and possibly even more advantageous to consider using the electrostatic engine in heliocentric space enroute to the target planet as well as after planetocentric space has been entered. Any judgment on how to interface a heliocentric interplanetary trajectory with planetary orbit insertion will have to be based upon further study which must involve optimizing the entire flight from earth orbit to the

desired final orbit about the target body. Figure 18 illustrates this type of problem. This involves the incoming parabolic trajectory, chemical retro-insertion into a very large eccentric ellipse, followed by the optimized spiraling transfer technique until the desired final orbit is obtained; in this case the final orbit is a small circular one.

It seems obvious that the slow spiral method of transferral would not be desirable for manned flights because of their long duration, but there are some instances where such an alternative might be preferred. For unmanned exploratory flights, where time may not be the most significant factor, this method offers an excellent chance to study the upper atmosphere of a given planet and to make planetary observations in a low, systematic manner. Starting in a large elliptical orbit, a spiral trajectory which steadily decreases in altitude until a low circular orbit is achieved might be desirable to record radiation, magnetic, and electrical fields at systematically decreasing altitudes, along with other upper level atmospheric conditions, planetary observations, etc. Orbital changes conducted by large impulse chemical retros make it impossible to record such long-time data as the transfers occur so quickly. There are many factors to consider when weighing the merits and drawbacks of optimized electrostatic propulsion (Reference 10).

The surface has only been scratched in this field. Improvements lie in many directions. For example, Handelsman (Reference 12) has put forth a formulation for the introduction of a switching function into the problem which would optimize transfer trajectories for minimum fuel and fixed-time

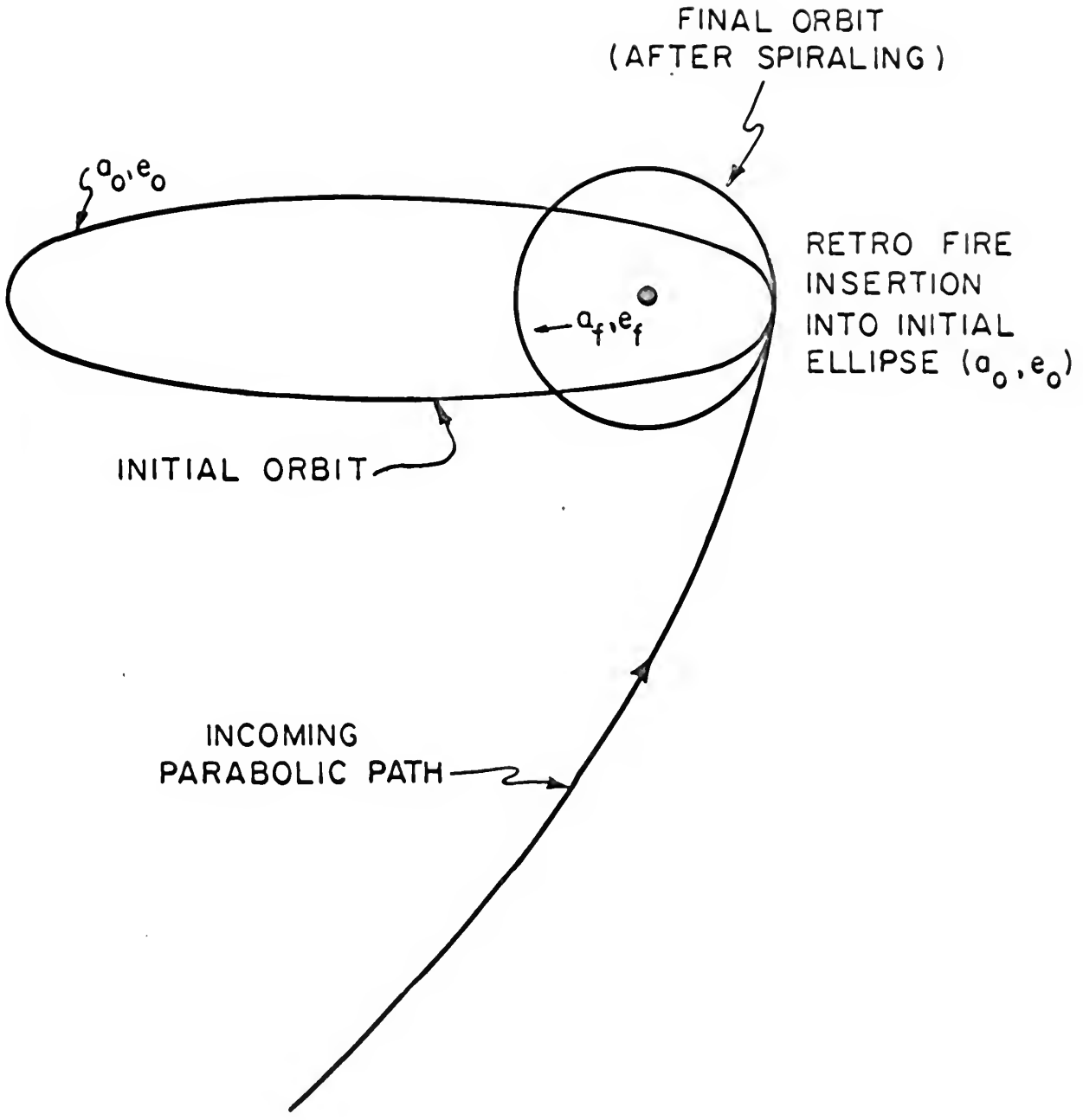


MARS RENDEZVOUS – SPIRAL TRANSFER

FIGURE 18

restraints. This would allow part of the trajectory to consist of coasting arcs in which the engine would be shut off by the switching function in order to comply with the fixed-time restraint.

Based upon the work done to date the following recommendations for further study are made.

1. Investigation of the occasional occurrence of negative eccentricities in certain transfer trajectories.

2. Use of a thrust acceleration which, for fixed-thrust magnitude, increases as the vehicle mass decreases due to fuel expenditure.

3. Optimization of the entire flight trajectory including interfacing with the rendezvous and final orbit insertion in order to find the best place to use electrostatic thrusting in the flight plan.

4. Study the solutions generated with a switching function for fixed-time problems and compare with solutions of the type covered in this thesis.

5. Addition of other orbital changes, such as rotation of apsidal line, non-planar transfers, etc.

6. Investigation of an analytic solution for a method of selecting the correct initial adjoint variables required for particular transfers desired. This would eliminate the guesswork now required at the outset of every problem. If this is not successful, iteration techniques may be necessary.

REFERENCES

1. Edelbaum, T. N., Optimum Low-Thrust Transfer Between Circular and Elliptic Orbits, Proc. 4th Nat'l Congr. Appl. Mech., California Meeting, June 1962, ASME, New York.

2. Edelbaum, T. N., Optimum Power-Limited Orbit Transfer in Strong Gravity Fields, AIAA J., 3, No. 5, May 1965, 921-925.

3. Edelbaum, T. N., Optimum Low-Thrust Rendezvous and Station-Keeping, AIAA J., 2, No. 7, July 1964, 1196-1201.

4. Handelsman, M., Optimal Fixed-Thrust Planetocentric Spiral Trajectories, STAR Memo No. 11, 17 March 1969, Princeton University.

5. Roy, A. E., The Foundations of Astrodynamics, MacMillan Company, New York, 1965.

6. Danby, J. M. A., Fundamentals of Celestial Mechanics, MacMillan Company, New York, 1962.

7. Elsgolc, L. E., Calculus of Variations, Pergamon Press Ltd., London, Addison-Wesley Publishing Company, Inc., Reading, Massachusetts, 1962.

8. Campbell, J. H., Lion, P. M., Shulzycki, A. B., TOPCAT 1: Trajectory Optimization Program - Case 2. Mars Rendezvous Mission (1980), 1 March 1968, Princeton University.

9. Hill, P. G., Peterson, C. R., Mechanics and Thermodynamics of Propulsion, 1965, Addison-Wesley Publishing Company, Inc., Reading, Massachusetts.

10. Jahn, R. G., Physics of Electric Propulsion, McGraw-Hill Book Company, New York, 1968.

11. Handelsman, M., Optimal Free-Space Fixed-Thrust Trajectories Using Impulsive Trajectories as Starting Iteratives, AIAA Journal, Vol. 4, No. 6, June 1966, pp. 1077-1082.

12. Handelsman, M., Minimum-Fuel Fixed-Thrust Planetocentric Elliptic Spiral Trajectories, STAR Memo No. 12, 14 May 1969.

13. Leitmann, G., Optimization Techniques, Academic Press, New York, 1962.

# APPENDIX A

## Description of Computer Program

This is a description of the computer program used for the numerical solution of optimal (minimum time and minimum E) planetocentric spiral trajectories using fixed power, fixed thrust propulsion, where the thrust acceleration is much less than the local gravitational acceleration. The program is written in Fortran IV computer language and incorporates a straightforward Runge-Kutta type integration process. It was designed for use on the 360/30 computer system, but can easily be adapted for use on other systems. Double precision was used in all program calculations (Reference 13).

In this appendix the important program input and output parameters are described, followed by the program itself and the program flow chart.

### Program Input Parameters

In order to produce a trajectory for optimal orbital transfer, certain initial quantities must be fed into the computer. These can be divided basically into three sets of values; the initial orbital conditions, the two Lagrangian variables ($\lambda_a$,$\lambda_e$), and the thruster conditions.

The initial orbital conditions include:

$a_o$ (initial semi-major axis)

$e_o$ (initial eccentricity)

k (mass constant)

$t_o = 0$ (transfer time)

$E_o = 0$ (eccentric anomaly)

$w_o = 0$ (angular position of line of apsides)

The thruster conditions include:

A (thrust acceleration)

M1 (number of revolutions desired)

M2 (number of steps per revolution)

The initial Lagrangian variables are:

$$\lambda_a(0) \equiv \lambda_{a_o}$$

$$\lambda_e(0) \equiv \lambda_{e_o}$$

The accuracy is determined by M2 (the number of steps per revolution desired). In other words, if M2 = 50, then the program will compute and print out the spacecraft's coordinates 50 times during each revolution, giving the exact description of the elliptical orbit which would be obtained were the engine to be cut off at any one of those points. However, we have found through experimentation that a value of M2 = 10 is sufficiently accurate and generates trajectories more quickly.

For every initial set of Lagrangian variables, a different transfer trajectory will be generated. The type of transfers generated are indicated in Figure 4.

Computer Output Parameters

At each point in the transfer trajectory a number of instantaneous quantities are printed out. These include the total step number, which, if divided by the number of steps per revolution, yields the number of revolutions to that point (a total step number of 156 would mean 15.6 revolutions at ten steps per revolution); the eccentric anomaly in radians; the thrust angle

in degrees; the $\xi$ function, which must go through zero for an optimal transfer to take place; the eccentricity; the change in eccentricity per radian of eccentric anomaly; the semi-major axis; the change in semi-major axis per radian of eccentric anomaly; the Lagrangian variable $\lambda_a$ and its change per radian; the Lagrangian variable $\lambda_e$ and its change per radian; the time elapsed since thrust initiation; the number of seconds of time per radian of eccentric anaomaly; angle of the line of apsides; the change in the line of apsides per radian of revolution.

# APPENDIX B

## Program Listing

```
C@@@     MAIN
      DOUBLE PRECISION W,X,Y,Z,A,GMU,N,D,H,SIGN
      COMMON           W,X,Y,Z,A,GMU,N,D,H,SIGN
      DOUBLE PRECISION H1(4),H2(4),H3(4),Q(7),QQ(7),DQ(7),DELQ(7),D1,D2,
     1 T, TT, PR(7)
      NAMELIST /INPUT/ M1,M2,A,GMU,Q,SIGN
      DATA Q / 7*0.D0 /
      SIGN = 1.D0
      DO 10 M = 1, 4
      H2(M) = 1.D0
      H1(M) = 0.5D0
   10 H3(M) = 0.5D0
      H1(3) = 1.D0
      H3(4) = 1.D0
      H3(1) = 0.D0
      H2(1) = H2(1) / 6.D0
      H2(4) = H2(1)
      H2(2) = H2(2) / 3.D0
      H2(3) = H2(2)
   20 READ(1,INPUT,END=200)
      IF( M1 ) 25, 200, 25
   25 WRITE(3,40) M1, M2, A, GMU , SIGN
   40 FORMAT( 1H1, I5, ' REVOLUTIONS', I5,' STEPS PER REV.  A = ',
     1 1PD15.8, ' MU = ',D15.8 ,'  SIGN =',D15.8 )
      WRITE(3,INPUT)
      T = 0.D0
      KMAX = IABS( M1 * M2 )
      Q(7) = Q(1)
      X = M2
      DT = 6.2831853071795865 / X
      KOUNT = 0
  100 TT = T
      DO 101 M = 1, 6
      PR(M+1) = Q(M)
      QQ(M) = Q(M)
  101 DELQ(M) = 0.D0
      DELQ(7) = 0.D0
      QQ(7) = Q(7)
      PR(1) = T * 57.2957795
      PR(6) = PR(6) / 86400.D0
      PR(7) = 0.D0
      IF(Q(6).NE.0.D0.OR.Q(7).NE.0.D0) PR(7) = DATAN2(Q(6),Q(7)    )
      PR(7) = PR(7) * 57.2957795
      WRITE(3,50) KOUNT, T, PR
   50 FORMAT( 1H0, I6,1P8D14.6 )
      CALL DERIV( T, Q, DQ  )
      PR(1) = DATAN2( N,D) * 57.2957795
      PR(2) = DQ(1)*Q(3) + DQ(2)*Q(4) - DQ(5)
      WRITE(3,51) PR(1), PR(2), (DQ(M),M=1,6)
   51 FORMAT( 1H ,  8X, 1P8D14.6 )
      KOUNT = KOUNT + 1
      K = 1
      GO TO 103
  102 K = 1 + K
      T = TT + DT * H3(K)
```

```
      CALL DERIV( T, Q, DQ )
103   D1 = H1(K) * DT
      D2 = H2(K) * DT
      DO 104 M = 1, 7
      DELQ(M) = DELQ(M) + D2 * DQ(M)
104   Q(M) = QQ(M) + DQ(M) * D1
      IF( K - 4 ) 102, 105, 102
105   DO 106 M = 1, 7
106   Q(M) = QQ(M) + DELQ(M)
      IF( KOUNT - KMAX ) 100, 107, 100
107   CALL DERIV( T, Q, DQ )
      DO 120 M = 1, 6
120   PR(M+1) = Q(M)
      PR(1) = T * 57.2957795
      PR(6) = PR(6) / 86400.D0
      PR(7) = 0.D0
      IF(Q(6).NE.0.D0.OR.Q(7).NE.0.D0) PR(7) = DATAN2(Q(6),Q(7))
      PR(7) = PR(7) * 57.2957795
      WRITE(3,50) KOUNT, T, PR
      PR(1) = DATAN2( N,D) * 57.2957795
      PR(2) = DQ(1)*Q(3) + DQ(2)*Q(4) - DQ(5)
      WRITE(3,51) PR(1), PR(2), (DQ(M),M=1,6)
      GO TO 20
200   RETURN
      END
```

```
C@@@    DERIV
      IMPLICIT REAL*8 ( A-H, O-Z )
      SUBROUTINE DERIV ( E, Q, DQ )
      DOUBLE PRECISION W,X,Y,Z,A,GMU,N,D,H,SIGN
      COMMON           W,X,Y,Z,A,GMU,N,D,H,SIGN
      DOUBLE PRECISION E,Q(4),DQ(4),DSIN,DCOS,DSQRT,DABS,SINE,COSE,
     1 COS2E, T1, T2, T3
      SQRTAU = DSQRT( Q(2) / GMU )
      SINE = DSIN( E )
      COSE = DCOS( E )
      COS2E = COSE * COSE
      Z = 1.D0 - Q(1) * Q(1)
      Y = DSQRT( DABS( Z ) )
      Z = Z * SINE
      X = Q(1) * SINE
      W = Y * (2.D0 * COSE - Q(1) * (COS2E+ 1.D0))
      N = 2.D0 * Q(2) * Q(4) * X + Q(3) * Z
      D = 2.D0 * Q(2) * Q(4) * Y + Q(3) * W
      H = DSQRT( N*N + D*D ) * SIGN
      T1 = X*N + Y*D
      T2 = Z*N + W*D
      T3 = A * Q(2) / GMU / H
      DQ(2) = 2.D0 * T3 * Q(2) * Q(2) * T1
      DQ(1) = T3 * Q(2) * T2
      DQ(5) = SQRTAU * (1.D0 - Q(1) * COSE)
      DQ(4) = -2.D0 * T3 * (3.D0 * Q(2) * Q(4) * T1 + Q(3) * T2 )
     1 + 1.5D0 * DQ(5)
      DQ(5) = DQ(5) * Q(2)
      DQ(3) = -T3*Q(2)*(2.D0*Q(2)*Q(4)*(N*SINE - Q(1)*D/Y) -
     1 Q(3)*(2.D0*X*N + (Q(1)*W/(Y*Y) + Y*(1.D0 + COS2E))*D))
     2 - SQRTAU * Q(2) * COSE
      DQ(6) = T3*Q(2)      *(Z*D/(Y*Y)*(2.D0-Q(1)*(COSE+Q(1))) -
     1 Y*N*(COSE - Q(1) ) )
      T3 = 0.D0
      IF(Q(6).NE.0.D0.OR.Q(7).NE.0.D0)T3 = DATAN2(Q(6),Q(7))
      T1 = DSIN(T3)
      T2 = DCOS(T3)
      DQ(7) = T2*DQ(1) - T1 * DQ(6)
      DQ(6) = T2*DQ(6) - T1*DQ(1)
      RETURN
      END
```

# APPENDIX C

## Program Flow Chart

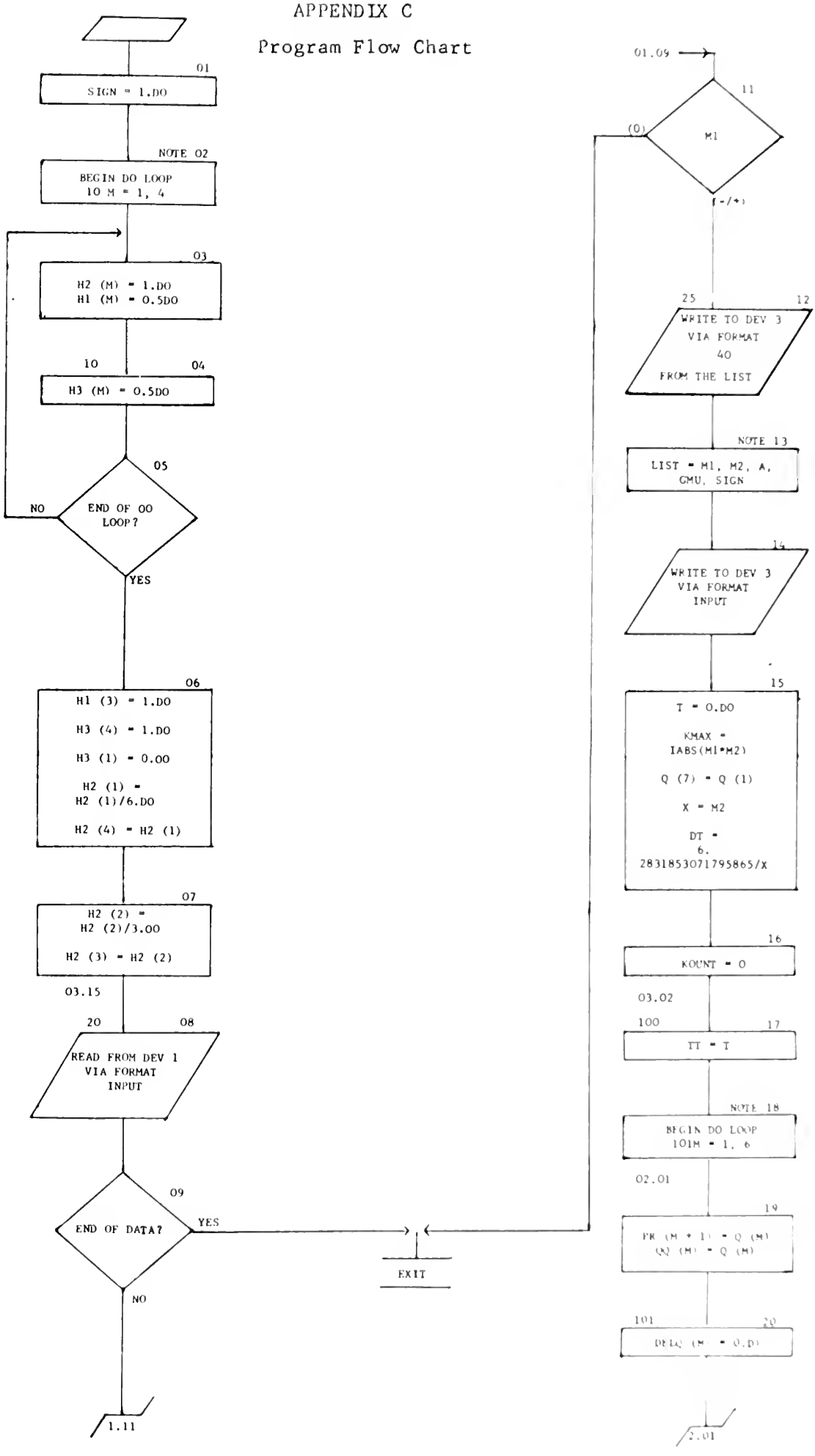

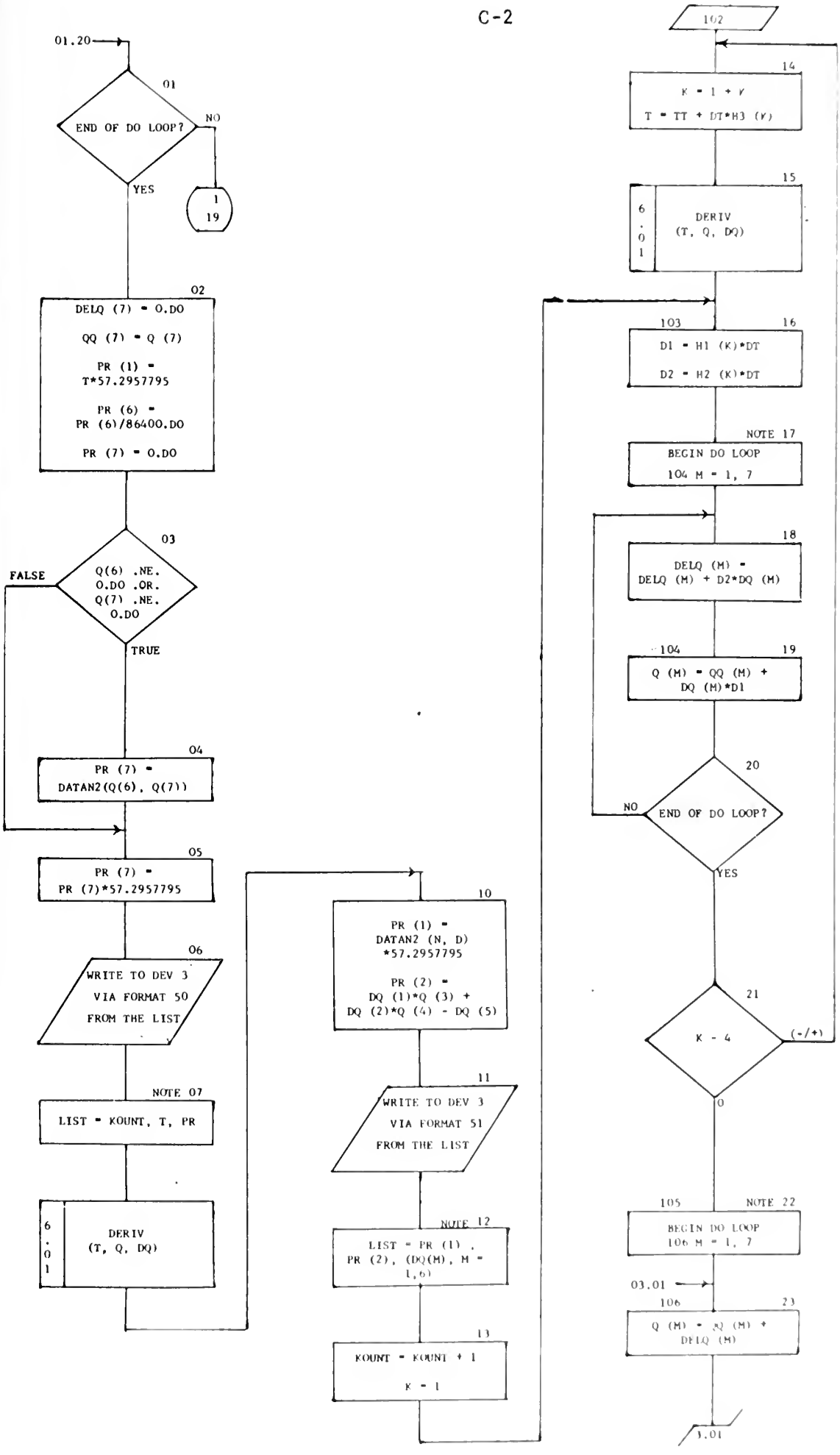
01.20
01
END OF DO LOOP?
NO
YES
1
19
02
DELQ (7) = 0.DO
QQ (7) = Q (7)
PR (1) = T*57.2957795
PR (6) = PR (6)/86400.DO
PR (7) = 0.DO
03
FALSE
Q(6) .NE. 0.DO .OR. Q(7) .NE. 0.DO
TRUE
04
PR (7) = DATAN2(Q(6), Q(7))
05
PR (7) = PR (7)*57.2957795
06
WRITE TO DEV 3 VIA FORMAT 50 FROM THE LIST
NOTE 07
LIST = KOUNT, T, PR
6.01
DERIV (T, Q, DQ)
10
PR (1) = DATAN2 (N, D) *57.2957795
PR (2) = DQ (1)*Q (3) + DQ (2)*Q (4) - DQ (5)
11
WRITE TO DEV 3 VIA FORMAT 51 FROM THE LIST
NOTE 12
LIST = PR (1), PR (2), (DQ(M), M = 1,6)
13
KOUNT = KOUNT + 1
K = 1
102
14
K = 1 + Y
T = TT + DT*H3 (Y)
15
6.01
DERIV (T, Q, DQ)
103
16
D1 = H1 (K)*DT
D2 = H2 (K)*DT
NOTE 17
BEGIN DO LOOP 104 M = 1, 7
18
DELQ (M) = DELQ (M) + D2*DQ (M)
104
19
Q (M) = QQ (M) + DQ (M)*D1
20
NO
END OF DO LOOP?
YES
21
K - 4
(-/+)
0
105
NOTE 22
BEGIN DO LOOP 106 M = 1, 7
03.01
106
23
Q (M) = QQ (M) + DELQ (M)
3.01

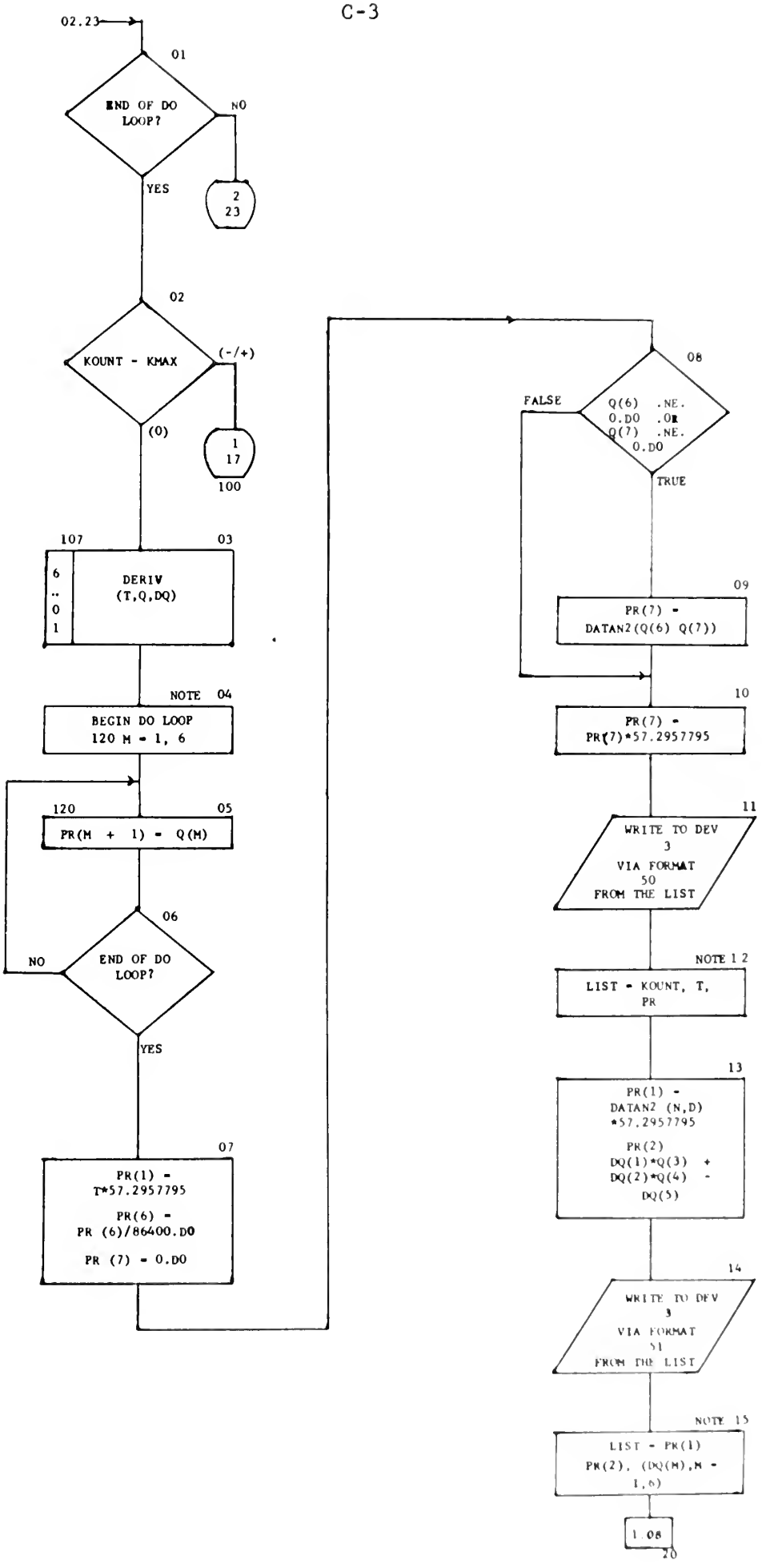
02.23
01
END OF DO LOOP?
NO
2 23
YES
02
KOUNT - KMAX
(-/+)
1 17
100
(0)
107
6 .. 0 1
03
DERIV (T,Q,DQ)
NOTE
04
BEGIN DO LOOP 120 M = 1, 6
120
05
PR(M + 1) = Q(M)
06
NO
END OF DO LOOP?
YES
07
PR(1) = T*57.2957795
PR(6) = PR (6)/86400.D0
PR (7) = 0.D0
08
FALSE
Q(6) .NE. 0.D0 .OR. Q(7) .NE. 0.D0
TRUE
09
PR(7) = DATAN2(Q(6) Q(7))
10
PR(7) = PR(7)*57.2957795
11
WRITE TO DEV 3 VIA FORMAT 50 FROM THE LIST
NOTE 12
LIST = KOUNT, T, PR
13
PR(1) = DATAN2 (N,D) *57.2957795
PR(2) DQ(1)*Q(3) + DQ(2)*Q(4) - DQ(5)
14
WRITE TO DEV 3 VIA FORMAT 51 FROM THE LIST
NOTE 15
LIST = PR(1) PR(2), (DQ(M),M = 1,6)
1.08
20

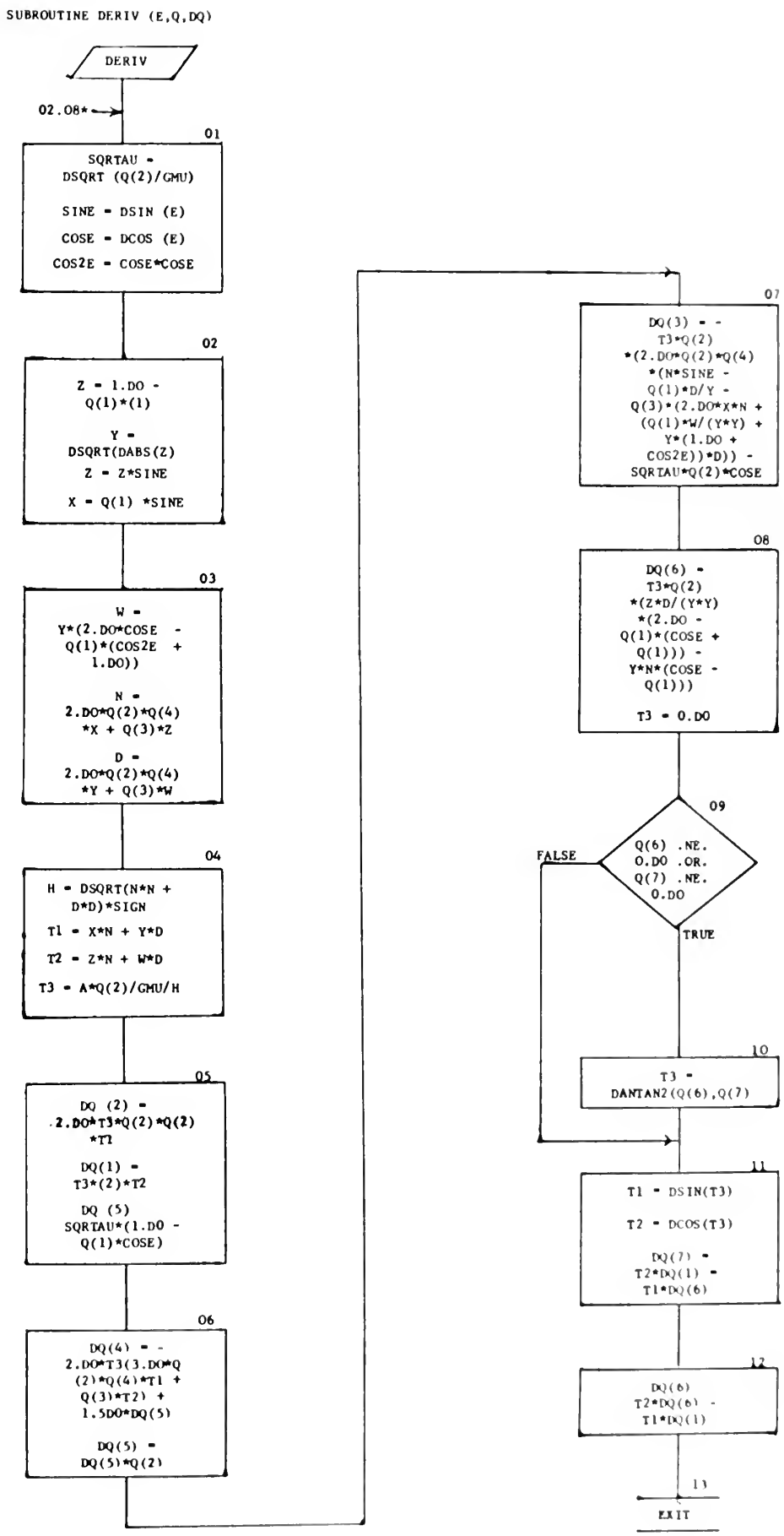
SUBROUTINE DERIV (E,Q,DQ)
DERIV
02.08*
01
SQRTAU =
DSQRT (Q(2)/GMU)
SINE = DSIN (E)
COSE = DCOS (E)
COS2E = COSE*COSE
02
Z = 1.DO -
Q(1)*(1)
Y =
DSQRT(DABS(Z)
Z = Z*SINE
X = Q(1) *SINE
03
W =
Y*(2.DO*COSE -
Q(1)*(COS2E +
1.DO))
N =
2.DO*Q(2)*Q(4)
*X + Q(3)*Z
D =
2.DO*Q(2)*Q(4)
*Y + Q(3)*W
04
H = DSQRT(N*N +
D*D)*SIGN
T1 = X*N + Y*D
T2 = Z*N + W*D
T3 = A*Q(2)/GMU/H
05
DQ (2) =
2.DO*T3*Q(2)*Q(2)
*T1
DQ(1) =
T3*(2)*T2
DQ (5)
SQRTAU*(1.DO -
Q(1)*COSE)
06
DQ(4) = -
2.DO*T3(3.DO*Q
(2)*Q(4)*T1 +
Q(3)*T2) +
1.5DO*DQ(5)
DQ(5) =
DQ(5)*Q(2)
07
DQ(3) = -
T3*Q(2)
*(2.DO*Q(2)*Q(4)
*(N*SINE -
Q(1)*D/Y -
Q(3)*(2.DO*X*N +
(Q(1)*W/(Y*Y) +
Y*(1.DO +
COS2E))*D)) -
SQRTAU*Q(2)*COSE
08
DQ(6) =
T3*Q(2)
*(Z*D/(Y*Y)
*(2.DO -
Q(1)*(COSE +
Q(1))) -
Y*N*(COSE -
Q(1)))
T3 = 0.DO
09
Q(6) .NE.
O.DO .OR.
Q(7) .NE.
0.DO
FALSE
TRUE
10
T3 =
DANTAN2(Q(6),Q(7)
11
T1 = DSIN(T3)
T2 = DCOS(T3)
DQ(7) =
T2*DQ(1) -
T1*DQ(6)
12
DQ(6)
T2*DQ(6) -
T1*DQ(1)
13
EXIT

# APPENDIX D

## Typical Computer Readout

The following page represents a computer read-out of a particular transfer trajectory generated by the minimum time program previously described. It was generated at a step size of ten per revolution, i.e., step ten is the end of the first revolution. Read across from the step desired. The meaning of each column is indicated at its head.

When reading across one will notice two lines of figures. In each case the second figure represents the change in value per radian of eccentric anomaly as the trajectory generates, with the exception that the second figure in the second column is the $\xi$ function which must go through zero for optimality. On this page of sample read-out the $\xi$ function does not yet go through zero. But later on in the trajectory it begins to oscillate through zero with every revolution.

```
 1000 REVOLUTIONS   10 STEPS PER REV.  A =  2.932341300-04 MU =  4.293000000 13  SIGN = 1.000000000 00
$INPUT
M1=        1000.M2=          10.A= 0.2932341299999999D-03.GMU=  429299999999999.99  ,Q= 0.0                  ,  3739999.999999999
  3429999.9999999339     , 0.1709999999999999D-01, 0.0                  , 0.0                  , 0.0                  ,SIGN=
 0.9999999999999999
$END                        E (degrees)       e                 a                 λ                 λ          t (days)          w (degrees)
  STEPS   E (radians)
      0  0.0              0.0               0.0               3.7403000 06  3.5000000 05  1.7100000-02  0.0               0.0
         0.0              -1.0247930 03  1.9108510-04  7.1465830 02 -1.0370130 03  3.9717060-04  1.1038930 03 -0.0

      1  6.2831850-01  3.6000000 01  1.1430550-04  3.7404430 06  3.4938960 05  1.7350680-02  8.0280290-03  9.5694450 00
         1.6461310 01 -1.0347250 03  1.6418970-04  6.8562270 02 -8.4230560 02  4.0250950-04  1.1039870 03  5.7338960-05

      2  1.2566370 00  7.2000000 01  1.9924910-04  3.7408350 06  3.4901040 05  1.7607510-02  1.6057140-02  1.9548360 01
         4.3700370 01 -1.0582690 03  1.0550060-04  5.1710570 02 -3.2307530 02  4.1577230-04  1.1041950 03  6.9343700-05

      3  1.8849550 00  1.0800000 02  2.5845060-04  3.7409770 06  3.4901020 05  1.7872660-02  2.4087930-02  1.9505810 01
         1.0389770 02 -1.0717250 03  1.0244300-04 -1.7149590 02  3.2069750 02  4.2617440-04  1.1044140 03 -4.8292080-05

      4  2.5132740 00  1.4400000 02  3.4240380-04  3.7406830 06  3.4938740 05  1.8139510-02  3.2119830-02  4.5174040 00
         1.5445840 02 -1.0589710 03  1.6380550-04 -6.4510760 02  8.4019340 02  4.2168620-04  1.1045010 03 -8.0728380-05

      5  3.1415930 00  1.8000000 02  4.5669730-04  3.7402470 06  3.4999740 05  1.8402830-02  4.0152070-02 -2.4783540-01
         1.8000000 02 -1.0507420 03  1.9119760-04 -7.1479980 02  1.0371390 03  4.1772250-04  1.1045060 03  8.2700330-07

      6  3.7699110 00  2.1600000 02  5.7094950-04  3.7398110 06  3.5060720 05  1.8666210-02  4.8183750-02  2.1991850 00
         -1.5423460 02 -1.0589360 03  1.6371250-04 -6.4367740 02  8.3970130 02  4.2187330-04  1.1043190 03  6.1315360-05

      7  4.3982290 00  2.5200000 02  5.5447940-04  3.7395210 06  3.5098410 05  1.8933150-02  5.6213160-02  4.7457970 00
         -1.0275290 02 -1.0712040 03  1.0144950-04 -1.5726400 02  3.2044650 02  4.2610660-04  1.1039040 03  2.8125880-06

      8  5.0265480 00  2.8800000 02  7.1339910-04  3.7396720 06  3.5098380 05  1.9197970-02  6.4239450-02  6.1317700-01
         -4.2827430 01 -1.0565840 03  1.0500350-04  5.2432330 02 -3.2295780 02  4.1483570-04  1.1035040 03 -1.1434170-04

      9  5.6548660 00  3.2400000 02  7.9813960-04  3.7400650 06  3.5060490 05  1.9454020-02  7.2263220-02 -4.3106060 00
         -1.6140120 01 -1.0323550 03  1.6399360-04  6.9651870 02 -8.4235240 02  4.0099490-04  1.1032090 03 -7.3821530-05

     10  6.2831850 00  3.6000000 02  9.1234850-04  3.7405090 06  3.4999440 05  1.9703630-02  8.0285440-02 -4.9688540 00
         -9.9789010-06 -1.0221890 03  1.9096260-04  7.1494970 02 -1.0371470 03  3.9532940-04  1.1031110 03  1.6540010-05

     11  6.9115040 00  3.9600000 02  1.0265690-03  3.7402530 06  3.4938390 05  1.9953180-02  8.8308260-02 -2.2916750 00
         1.6052900 01 -1.0133750 03  1.6401980-04  6.9743530 02 -8.4254900 02  4.0078960-04  1.1033980 03  9.3078870-05

     12  7.5398230 00  4.3200000 02  1.1112870-03  3.7413490 06  3.4900450 05  2.0209050-02  9.6334770-02  1.5860160 00
         4.2180220 01 -1.0569240 03  1.0475990-04  5.3056800 02 -3.2337460 02  4.1452160-04  1.1041100 03  1.1203340-04

     13  8.1681400 00  4.6800000 02  1.1494810-03  3.7415090 06  3.4930430 05  2.0473810-02  1.0436720-01  3.5638850 00
         1.0073130 02 -1.0725410 03  1.0037500-04 -1.3245070 02  3.2099570 02  4.2643560-04  1.1049600 03 -1.0961900-05

     14  8.7964590 00  5.0400000 02  1.2528190-03  3.7412270 06  3.4938150 05  2.0741350-02  1.1240510-01  1.5547340 00
         1.5342870 02 -1.0515330 03  1.6366750-04 -6.3956810 02  8.4024440 02  4.2332770-04  1.1055560 03 -7.0335710-05

     15  9.4247780 00  5.4000000 02  1.3671770-03  3.7407920 06  3.4999140 05  2.1005810-02  1.2044600-01  3.5263120-01
         1.8000000 02 -1.0537770 03  1.0142770-04 -7.1511180 02  1.0374080 03  4.1951670-04  1.1057530 03 -1.1782380-06

     16  1.0053100 01  5.7600000 02  1.4815120-03  3.7403580 06  3.5060150 05  2.1270330-02  1.2848620-01  1.1947280 00
         -1.5324650 02 -1.0414010 03  1.5356180-04 -6.3804570 02  8.3975370 02  4.2351190-04  1.1053750 03  6.2078680-05

     17  1.0681410 01  6.1200000 02  1.5665870-03  3.7400780 06  3.5097850 05  2.1537050-02  1.3652160-01  2.2515720 00
         -2.0585550 01 -1.0232360 03  9.0641470-05 -1.1706270 02  3.2068030 02  4.2532700-04  1.1044620 03 -2.3986690-06

     18  1.1309730 01  6.4800000 02  1.6522560-03  3.7403490 06  3.5097820 05  2.1802360-02  1.4454980-01  4.5916670-01
         -4.1364130 01 -1.0051470 03  1.0425190-04  5.3720360 02 -3.2325260 02  4.1357070-04  1.1034500 01 -1.1779360-06
```